Euclid meets CMB lensing:

First cosmological constraints from the Euclid Quick Data Release

Colloque national du WG Dark Energy, 2-4 Nov 2026

Margherita Lembo - Institut d'Astrophysique de Paris

First cosmological results from Euclid

Astronomy & Astrophysics manuscript no. output
October 19, 2026
©ESO 2026

Euclid Quick Data Release (Q1)

Clustering of photometrically selected galaxies and their cross-correlation with cosmic microwave background lensing

Euclid Collaboration: G. Fabbian[⋆1,2,3], L. Legrand[1,4,5], M. Lembo[6], L. Pagano[7,8], G. Piccirilli[9], R. Kou[10,11], K. Benabed, W. D'Assignies, S. Gouyou Beauchamps, W. Hartley, N. Tessore, and I. Tutusaus

Under Euclid internal review

ABSTRACT

We perform a tomographic measurement of the clustering of a magnitude-limited galaxy sample from the Euclid Q1 data release and its cross-correlation with cosmic microwave background (CMB) lensing from *Planck* and the Atacama Cosmology Telescope (ACT). The measurements are consistent across the three Euclid Q1 fields, with a combined detection significance exceeding 30σ over a total sky area of ~ 60 deg^2. We verify their robustness against a range of potential contaminants and systematic effects providing a characterisation of the galaxy bias as well as an assessment of the quality of the photometric redshift estimates. These findings are then used to carry out a cosmological analysis accounting for galaxy bias modelling and redshift uncertainties from the combination of galaxy clustering and CMB lensing cross-correlation. Using a D_G statistic, less prone to systematic effects, we obtain an amplitude of the growth factor $A_D = 0.84 \pm 0.16$. Furthermore, assuming priors on linear and non-linear galaxy bias parameters obtained from the *Euclid* Flagship 2 simulation, we obtain $\Omega_\mathrm{m} = 0.282^{+0.059}_{-0.078}$ and $\sigma_8 = 0.826 \pm 0.028$ from a full likelihood analysis. All these results are consistent with recent results in the literature based on ACT, *Planck*, DES-Y3, unWISE and DESI LRGs and reach a comparable sensitivity despite using substantially less sky area. Our analysis also shows that including CMB lensing cross-correlation improves the constraining power by up to 30% compared to an analysis based on galaxy clustering alone, and yields a better fit to the data. Even at this initial phase of the data analysis, our findings demonstrate the strong potential of *Euclid* to deliver precise cosmological constraints in its future data releases, and highlight the effectiveness of CMB lensing cross-correlations at mitigating *Euclid*'s systematic effects and enhancing the mission's constraining power.

Key words. Cosmology: observations; large-scale structure of Universe; cosmic background radiation; cosmological parameters; Surveys.


G. Fabbian


L. Legrand

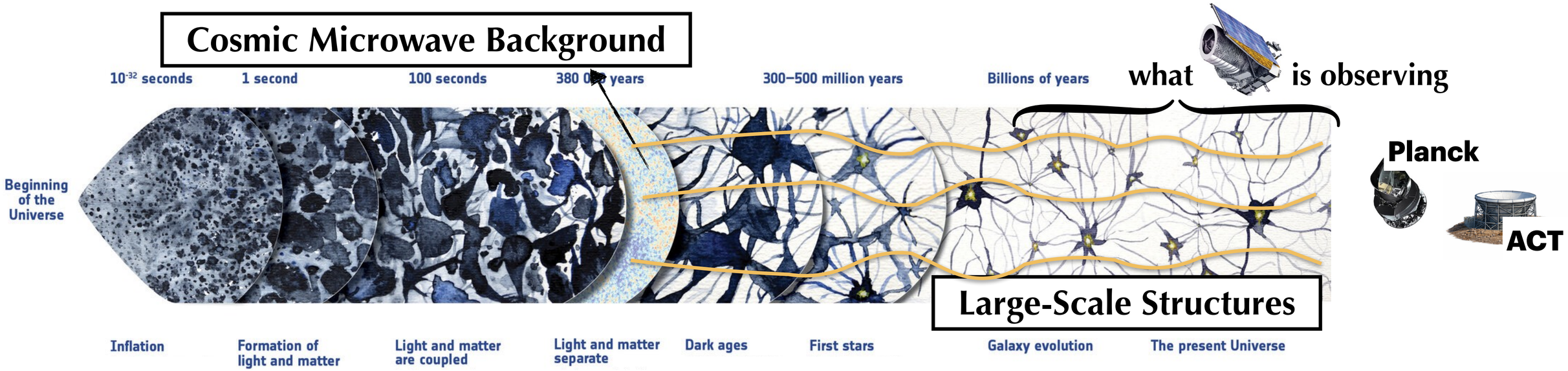

M. Lembo


R. Kou


G. Piccirilli


L. Pagano

Why Euclid × CMB?



CMB is the most distant light: **CMB photons cross large-scale structures** as they form

CMB lensing → gravitational lensing of CMB photons by all matter along the line of sight

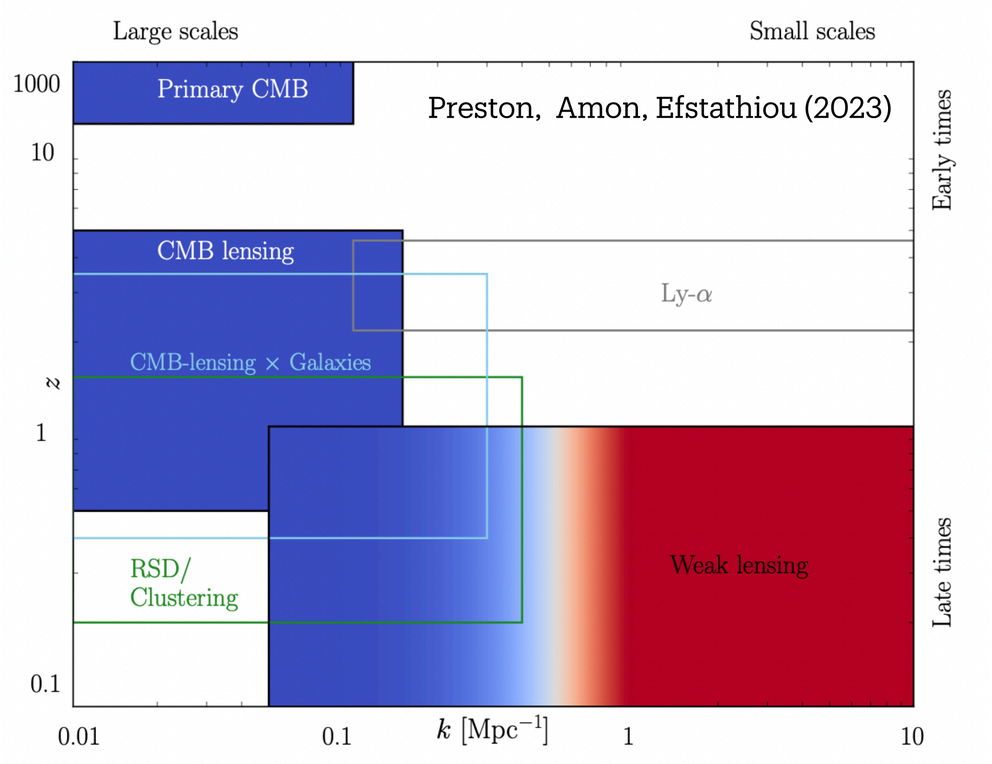
CMB temperature (ISW) → decay of gravitational potentials on the largest scales, imprinted on CMB photons

Thermal SZ (tSZ) → inverse Compton scattering by hot intracluster electrons; traces hot gas

Kinetic SZ (kSZ) → inverse Compton scattering by bulk electron flows; traces gas momentum

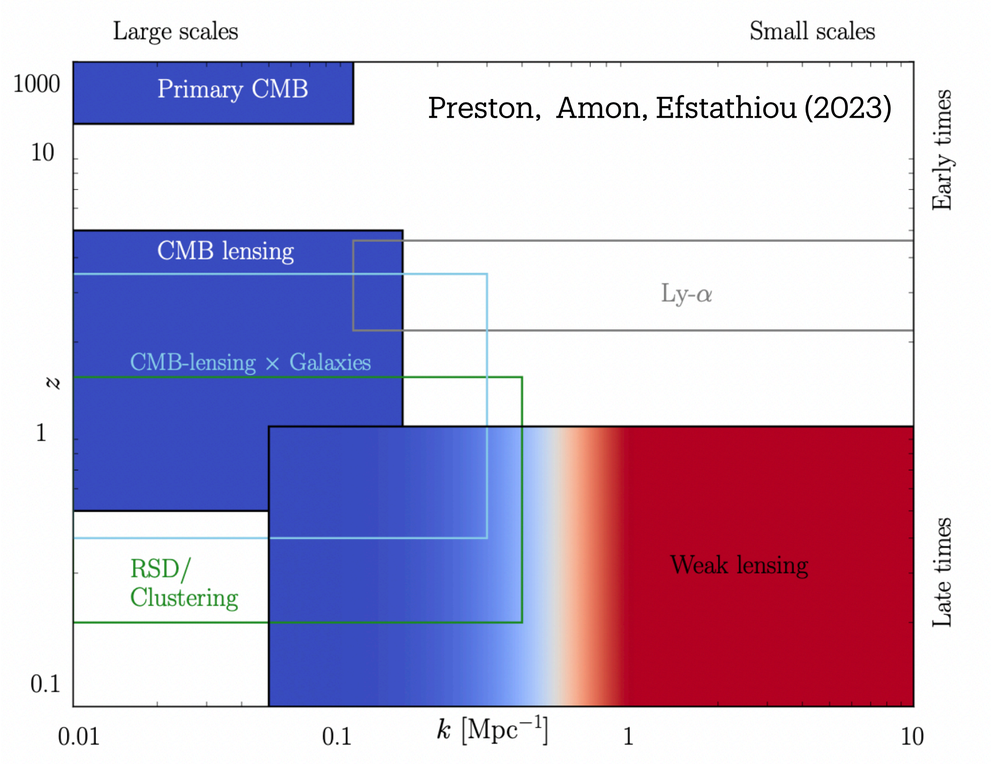
Why Euclid × CMB?

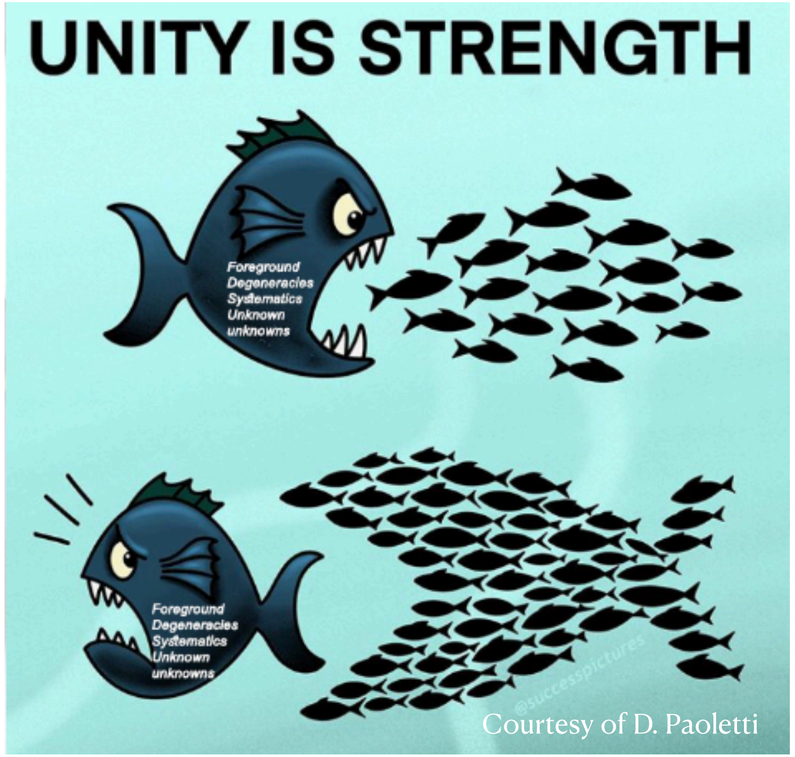
CMB and LSS probe the **same Universe**
at **different epochs and scales**



Why Euclid × CMB?

CMB and LSS probe the **same Universe** at **different epochs and scales**

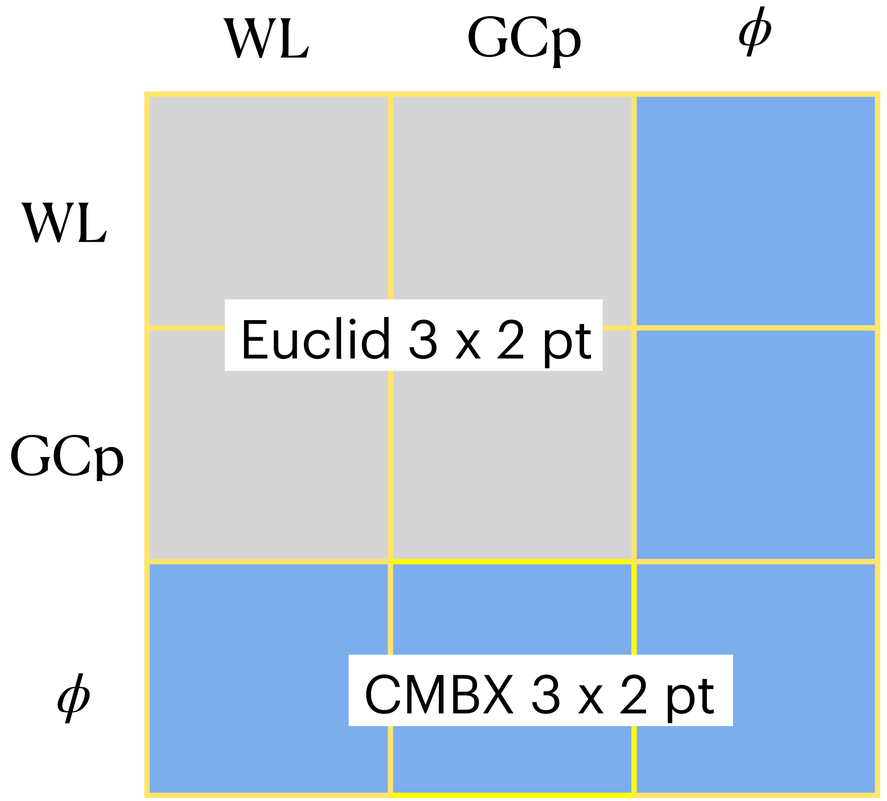




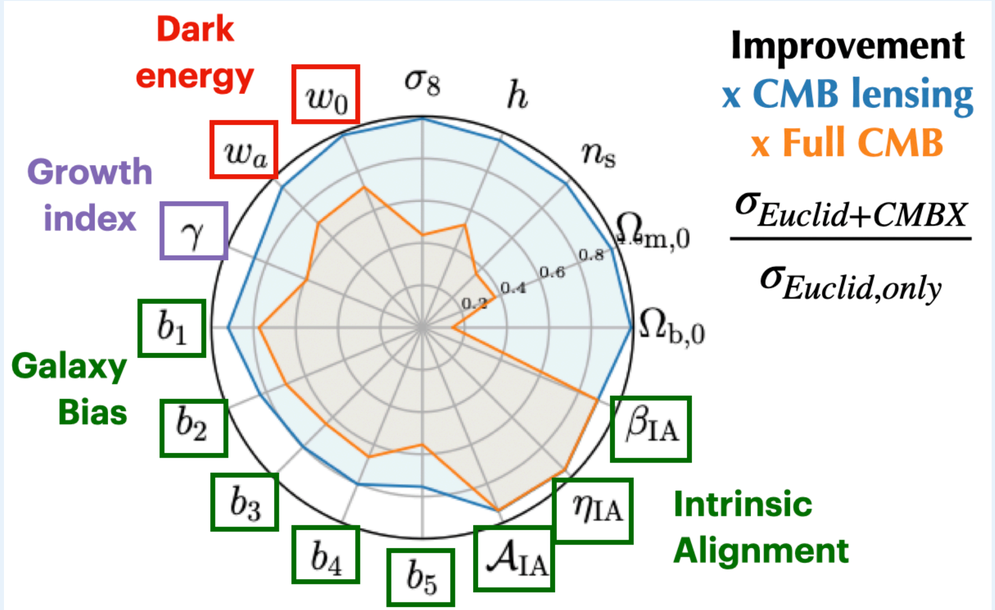
Different probes, **different systematics**: together they are more robust

Euclid × CMB: 6x2pt analysis

$$C_\ell^{XY} = L^A(\ell)L^B(\ell) \int \frac{\mathrm{d}z}{H(z)\chi^2(z)} W_i^X(z) W_j^Y(z)\, P_m\left(\frac{\ell + 1/2}{\chi(z)}, z\right) + N_\ell^{XY}$$



Forecasts: Euclid DR3 and SO-like CMB data



Euclid collab. w/ **CMBX SWG** (Ilic+21)

First “quick” data release



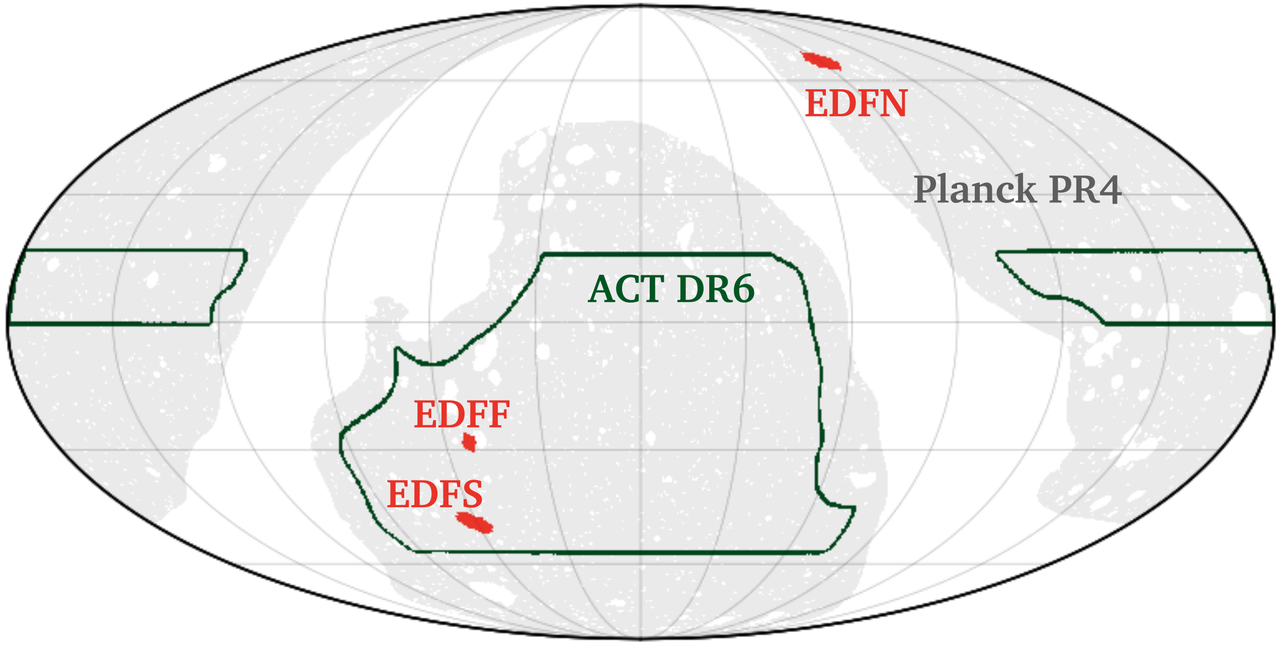
Euclid Consortium
A space mission to map the Dark Universe

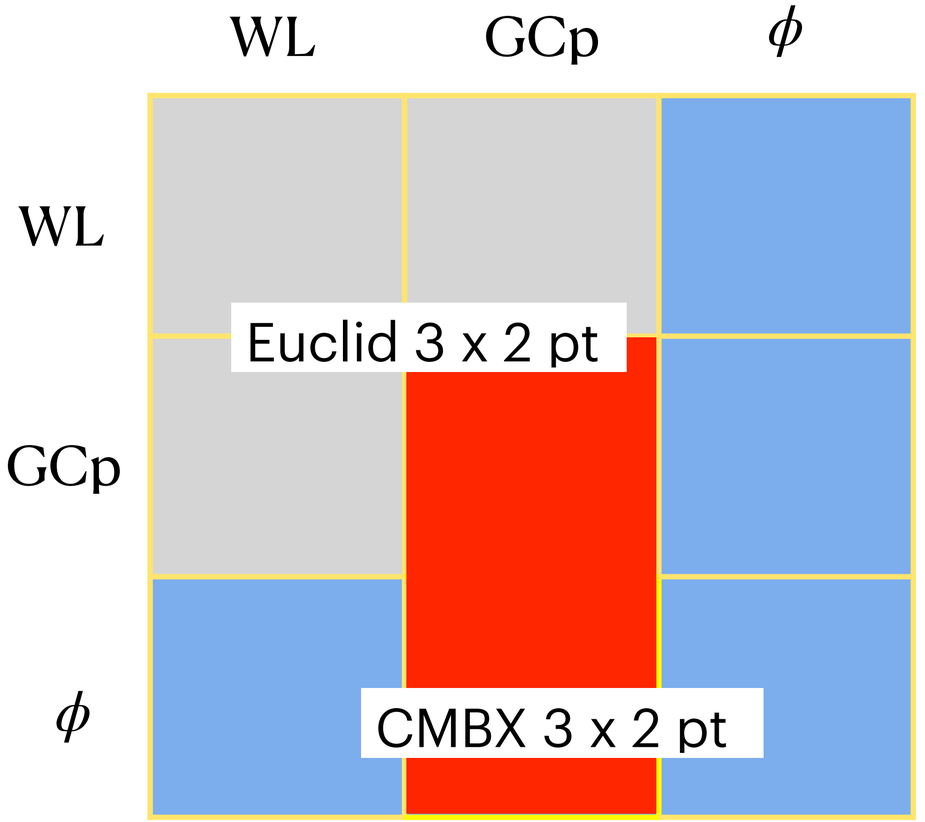
The Mission | News & Media | For Scientists | The Consortium | The Euclid Blog

Euclid data release: Q1

Euclid has a number of planned data releases to the world. The first one is the “Quick Data Release 1” or Q1 for short, that released 63.1 deg^2 of wide-survey science data on 19 March 2025. This release, containing approximately 26 million detections, is not a cosmology release but primarily aimed at a variety of astrophysical studies, providing VIS and NISP images, NISP spectroscopy, external ground-based data, catalogues, and masks. A total of seven technical publications and a supplement describe the content of the release. An overview is given in *Euclid Collaboration: Aussel et al., 2025*, “Euclid Quick Data Release (Q1) – Data release overview”. A constantly updated list of Q1 reference and science papers is given below. Complete information is available at ESA’s Q1 data release page, with a detailed description in the release’s Explanatory Supplement, and with a specific pointer to the Release Notes.

Euclid Q1 × CMB: 2x2pt analysis

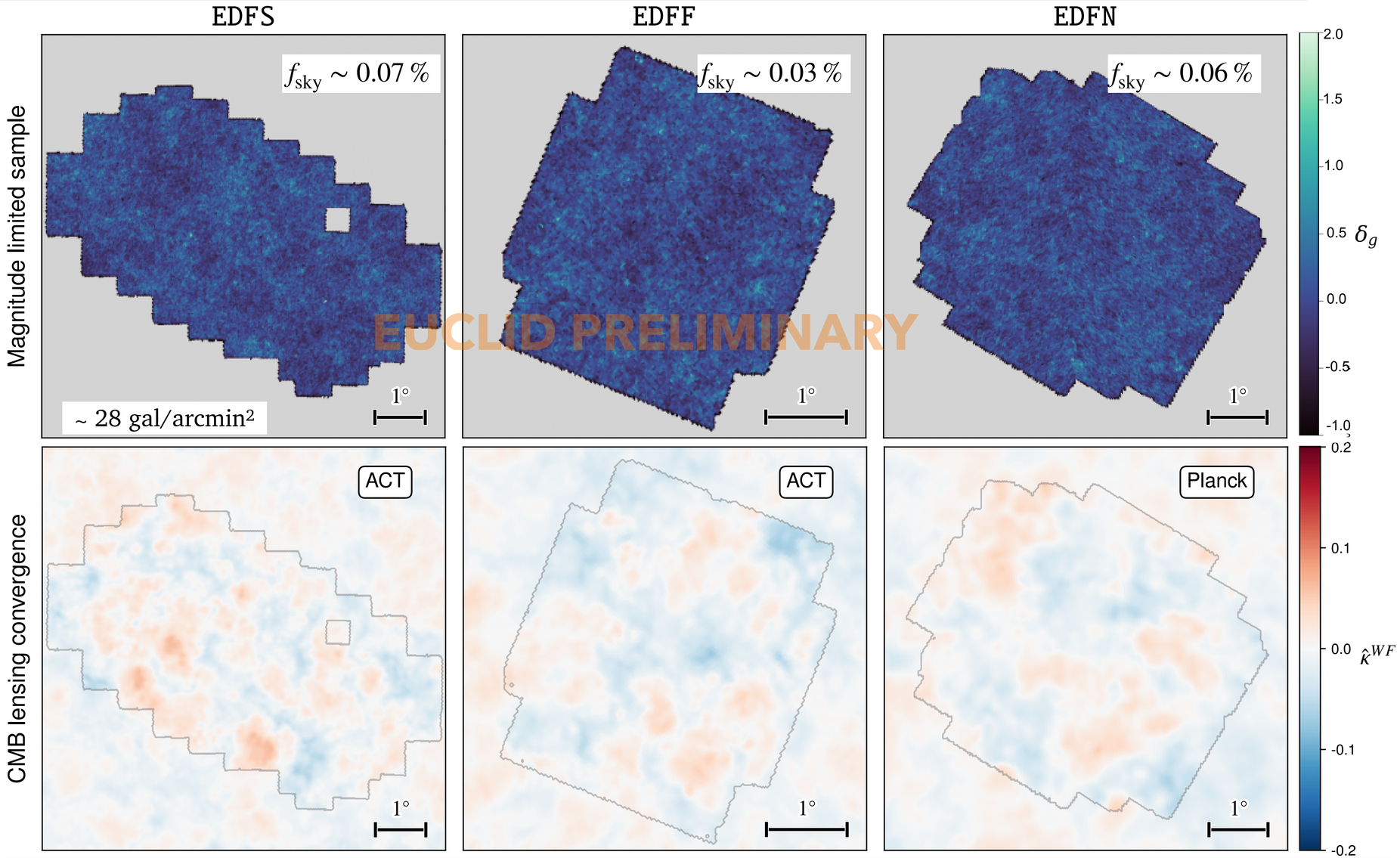




Euclid Q1 (~63 deg^2): EDFN + EDFF + EDFS

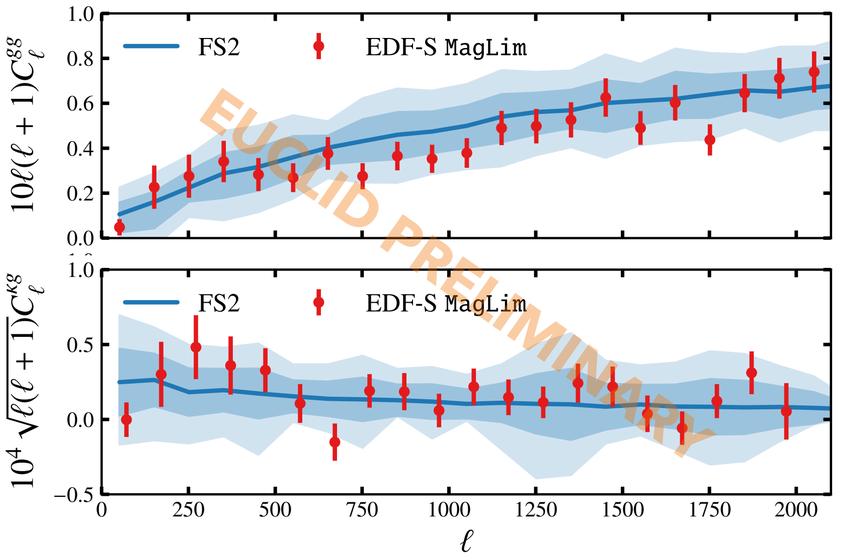
- ✓ EDFN x **Planck** only
- ✓ EDFF/EDFS x **Planck** and **ACT**

Euclid Q1 maps



Comparison with Flagship 2 simulation

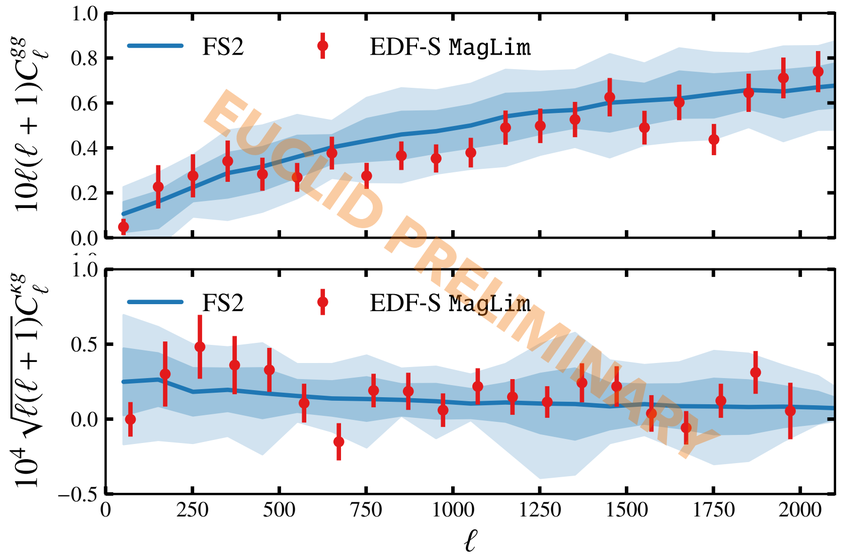
- **No tomography:** properties consistent across fields
- In **agreement** with “uncalibrated” FS2 simulation (PTE>0.08) using all scales

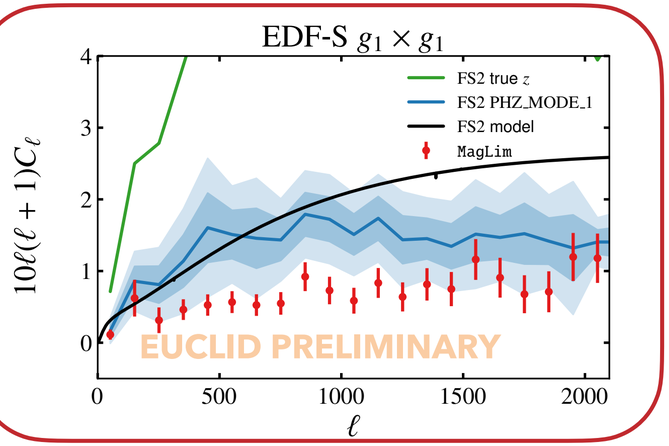


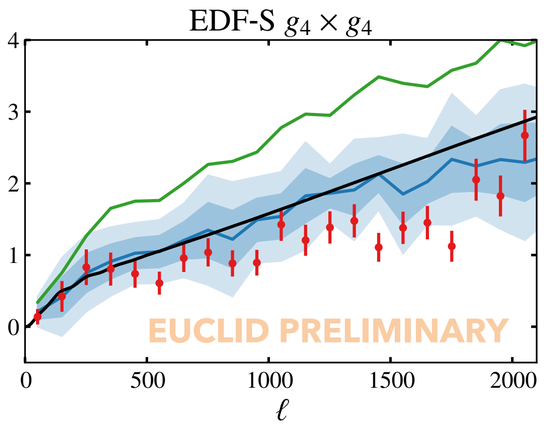
Comparison with Flagship 2 simulation

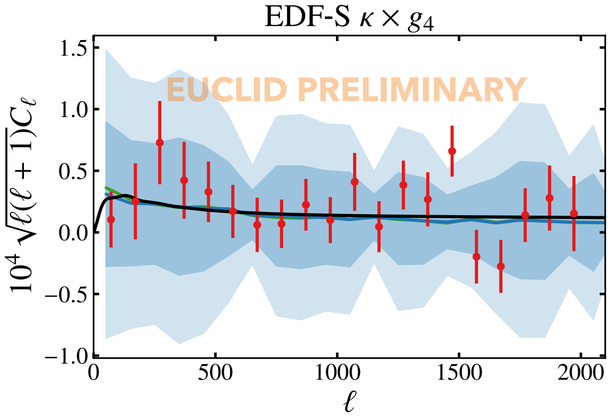
- **No tomography:** properties consistent across fields
- In **agreement** with “uncalibrated” FS2 simulation (PTE>0.08) using all scales

- **Tomography is harder** because of redshift errors, bias evolution…
- Fiducial model reproduces FS2 on relevant scales
- From FS2: **CMBX immune to redshift errors**

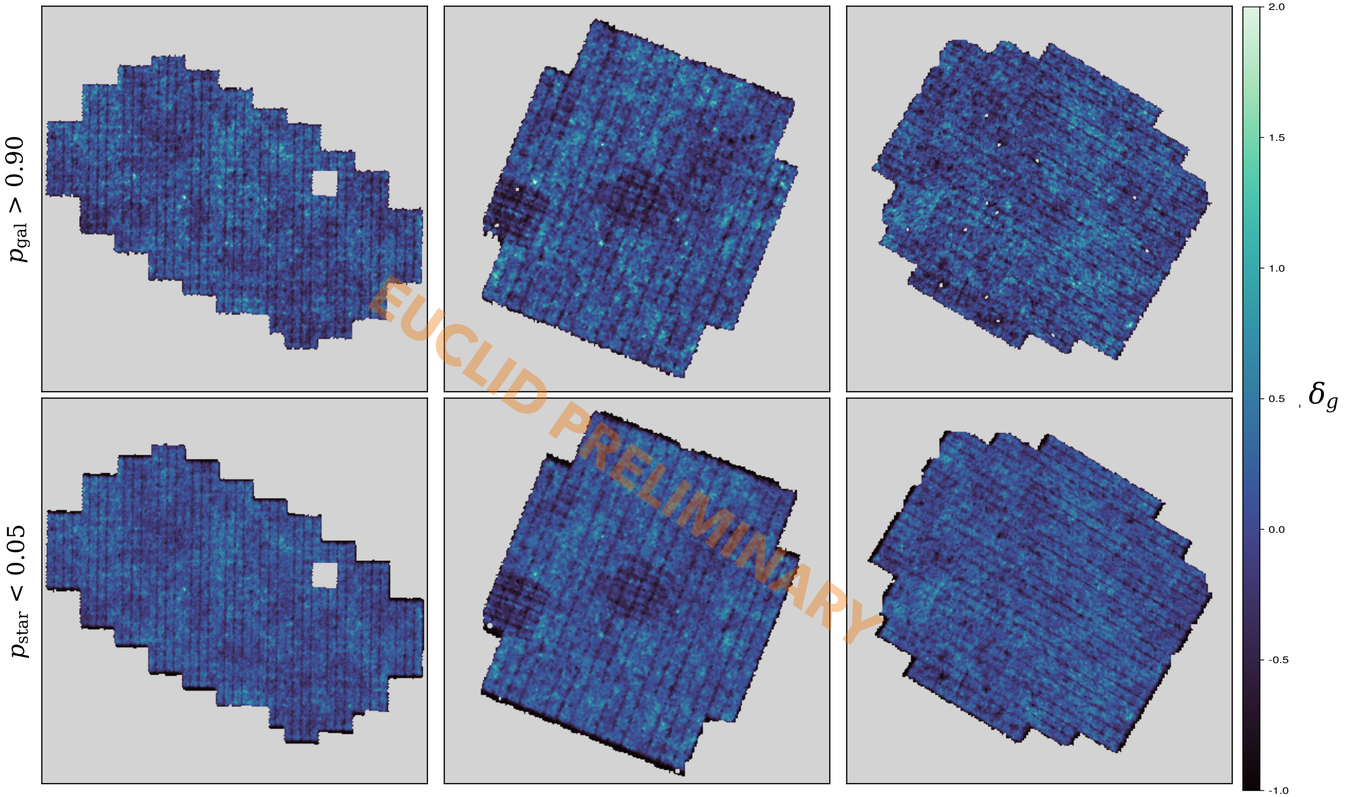


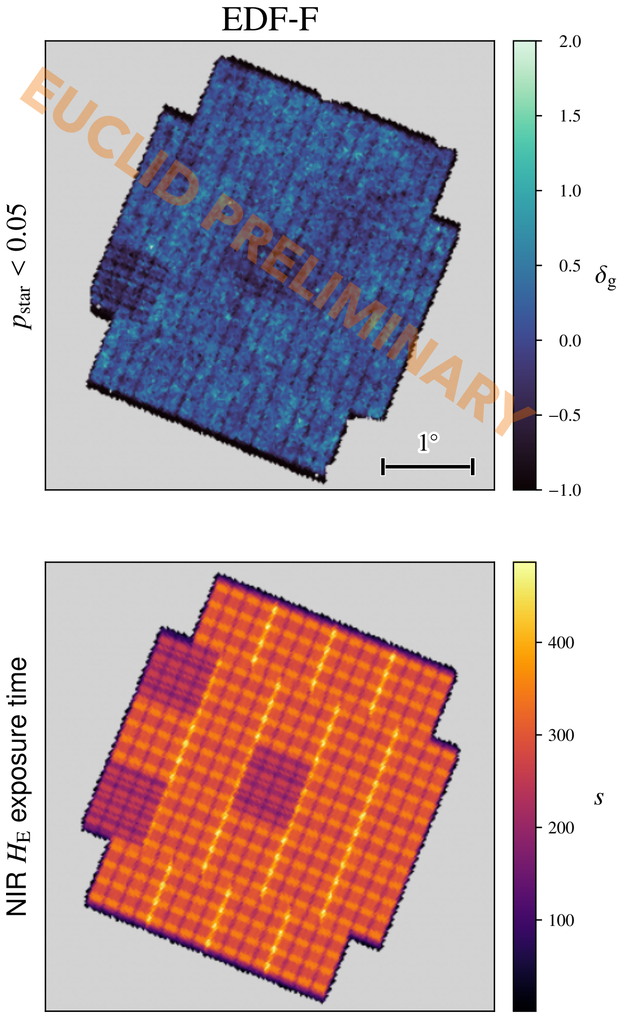






Where do systematics show up?

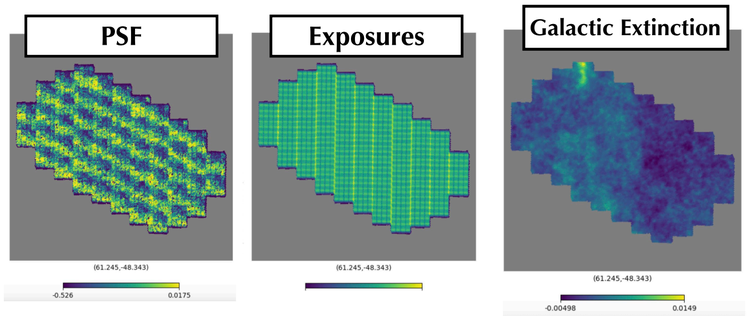




Two different sample selection based on purity of galaxy classification or star classification rejection respectively. The two cuts deliver samples with:

$$p_{\rm gal} = 11\ {\rm gal/arcmin^2} \text{ and } p_{\rm star} = 21\ {\rm gal/arcmin^2}$$

Imaging systematic treatment

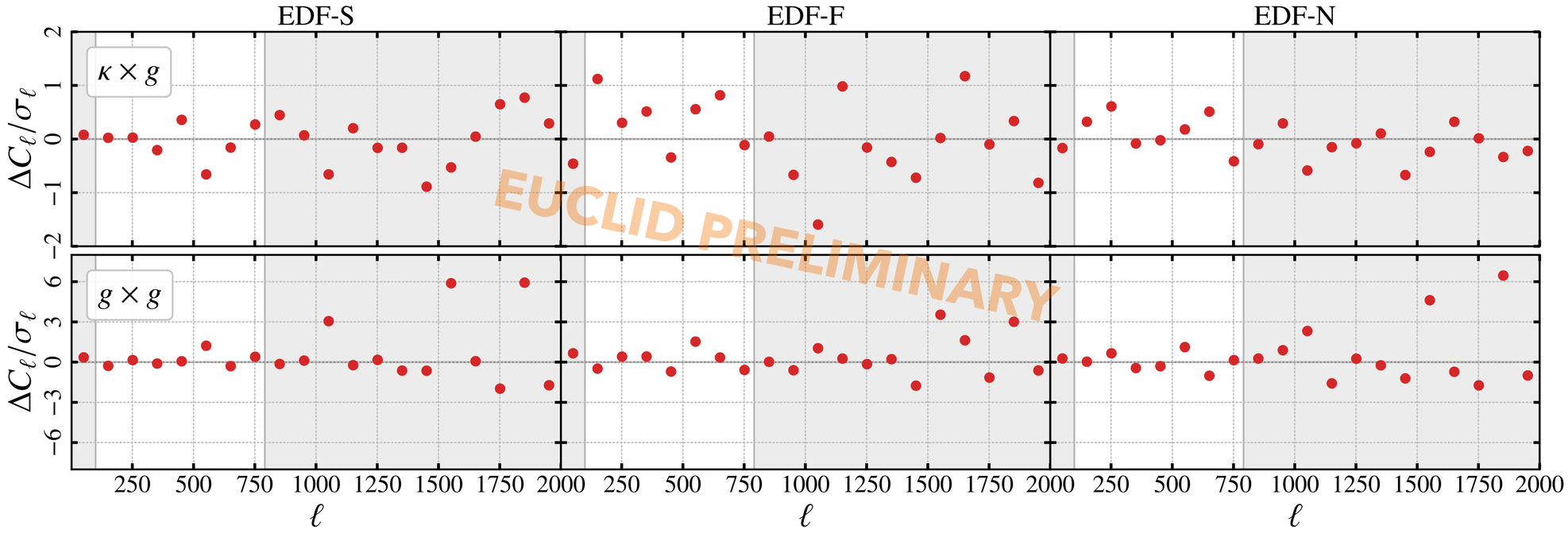


+12 others

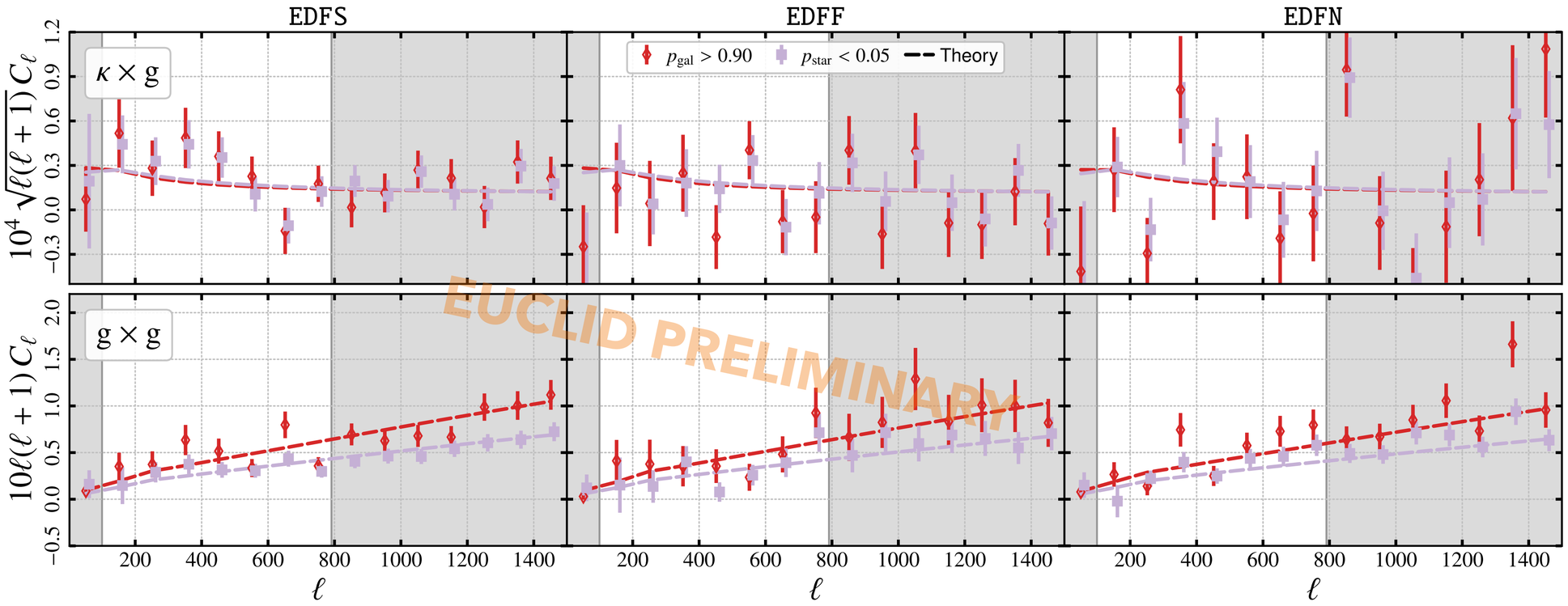
Linear deprojection

Minor effects in the science band on well defined scales

No effect on κg



Power spectra



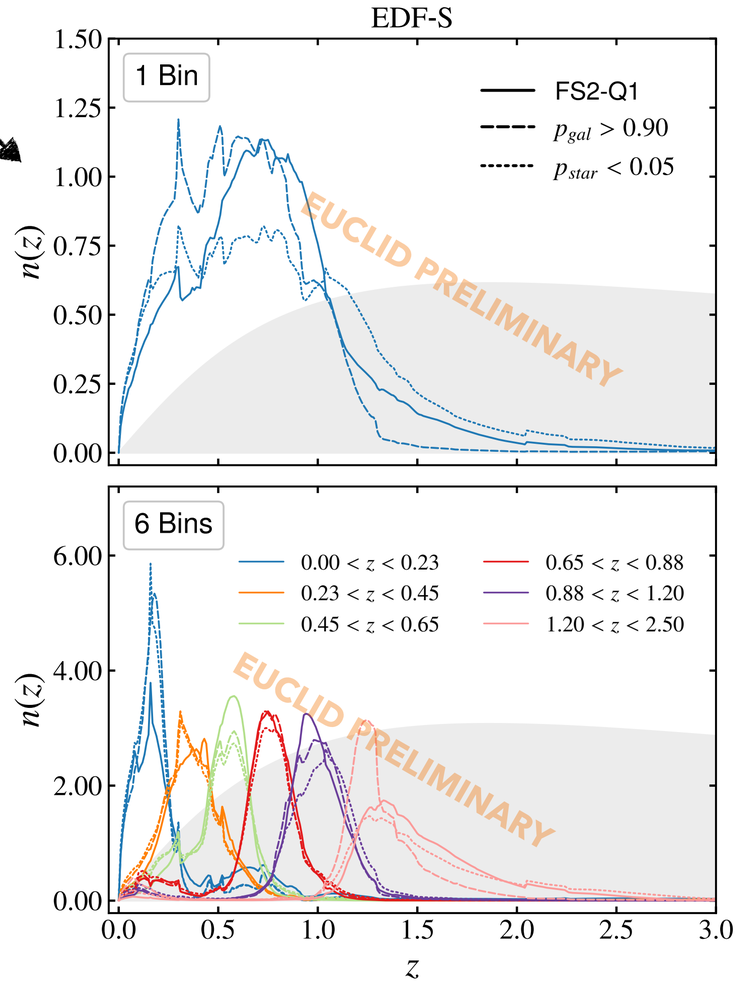
S/N above 20 for kg alone in the 6bin case and combining 3 ED fields

- Theory lines **not a fits**!

  ➡Planck 2018 + estimated $n(z)$ + fiducial Flagship calibrated galaxy bias model
- **Good agreement in the single-bin case**, at fixed model, with no parameters fitted
- **Tomography (6 bins) is harder** at face value: some tensions at fixed model, driven by photo-z errors

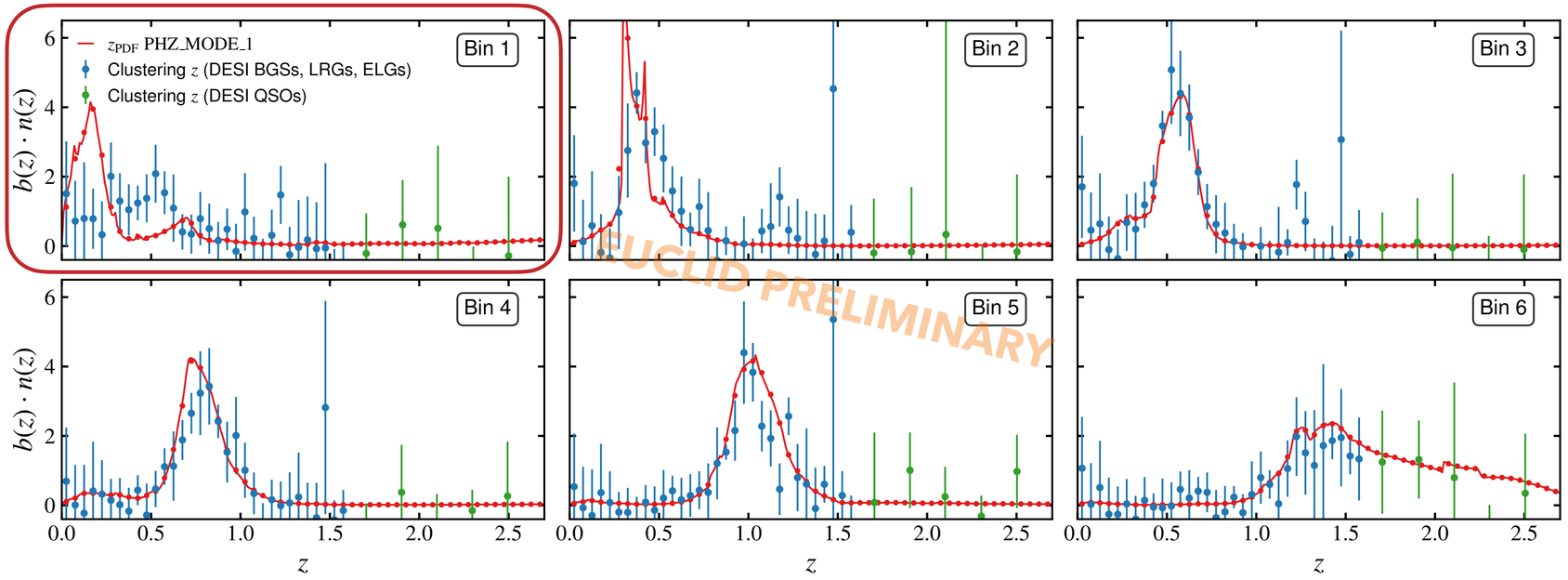
Redshift distribution, $n(z)$

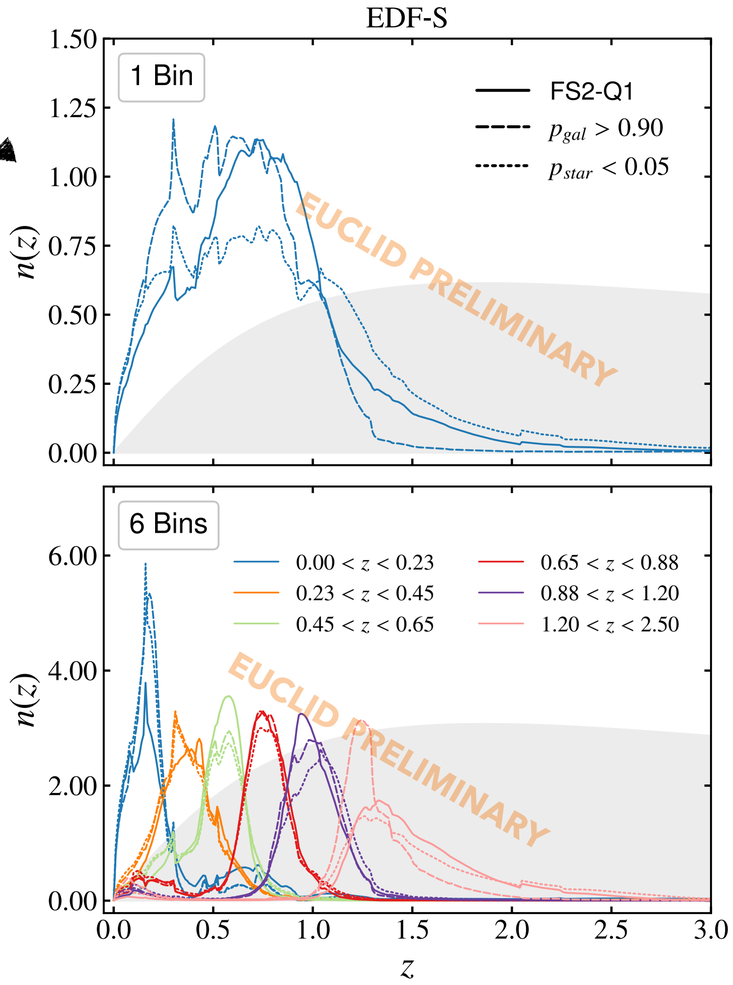
- For each redshift bin, the $n(z)$ is estimated from stacking of the galaxy's photo-z PDF
- EDFS and EDFF are consistent, while EDFN is not: **different external photometric data**
- $n(z)$ in **"good agreement"** with FS2



$n(z)$ vs clustering redshift

- For each redshift bin, the $\mathrm{d}N/\mathrm{d}z$ is estimated from stacking of the galaxy's photo-z PDF
- EDFS and EDFF are consistent, while EDFN is not: **different external photometric data**
- $n(z)$ in **"good agreement"** with FS2
- **Clustering redshifts** with DESI show robustness (only 10deg^2, more available for DR1)





Galaxy bias modelling

Galaxy bias modelled using Eulerian perturbation theory at 1-loop order:

$$g = b_g\, b_1^{\rm fid}\, \delta_m + b_g^{nl} \frac{b_2^{\rm fid}}{2} \delta_m^2 + \frac{b_s}{2} s^2 + \frac{b_{3\rm nl}}{2} \psi_{\rm nl} + \frac{b_{k2}}{2} \nabla^2 \delta_m \qquad b_s = -\frac{4}{7}(b_g\, b_1^{\rm fid} - 1)$$

Saito+2014;
Gil-Marín+2015;
Pandey+2020

Fiducial bias parameters calibrated from Euclid Flagship simulations

Higher-order bias parameters set to zero

Second-order non-local (tidal) bias fixed using the co-evolution relation

Model validated on FS2 simulation up to $k_{\rm max} = 0.5h/{\rm Mpc}$:

- ➡ $b_g = 0.983 \pm 0.012$
- ➡ $b_g^{nl} = 0.99 \pm 0.17$

Science bands

z bins	Redshift range	$\ell_{\rm min}$	$\ell_{\rm max}(k_{\rm NL})$	$\ell_{\rm max}(k_{\rm max})$
1bin	$0.00 < z < 2.50$	100	372	791
6bins	$0.00 < z < 0.23$	100	144	367
	$0.23 \leq z < 0.45$	100	220	526
	$0.45 \leq z < 0.65$	100	301	675
	$0.65 \leq z < 0.88$	100	445	898
	$0.88 \leq z < 1.20$	100	625	1128
	$1.20 \leq z < 2.50$	100	846	1353

Towards a full cosmological inference

Parameter	Value
Cosmological parameters	
$\Omega_{\rm m}$	$\mathcal{U}(0.01, 0.95)$
$\ln\left(10^{10} A_{\rm s}\right)$	$3.047 \quad \vert \quad \mathcal{U}(1.0, 5.0)$
$\Omega_{\rm m} h^3$	0.09635
$\Omega_{\rm b} h^2$	0.02242
$\Omega_\nu h^2$	0.00064
n_s	0.9665
$\sum m_\nu$	0.06 eV
τ	0.0561
h	derived $\left(\left[\Omega_{\rm m} h^3 / \Omega_{\rm m}\right]^{1/3}\right)$
$\Omega_{\rm c} h^2$	derived $\left(\Omega_{\rm m} h^2 - \Omega_{\rm b} h^2 - \Omega_\nu h^2\right)$
Nuisance parameters	
$\Delta_z^{(i)}$	$\mathcal{N}(0, 0.1)$
$b_{\rm g}$	$\mathcal{U}(0.1, 3.0) \quad \vert \quad \mathcal{N}(1.0, 0.036)$
$b_{\rm g}^{\rm nl}$	$\mathcal{N}(1.0, 0.2)$
b_1	derived $\left(b_{\rm g} b_1^{\rm fid}\right)$
b_2	derived $\left(b_{\rm g}^{\rm nl} b_2^{\rm fid}\right)$
b_{s^2}	derived $(-4/7\,[b_1 - 1])$

sampled cosmological parameters

redshift errors, $n^i(z) \rightarrow n^i(z + \Delta_z^i)$

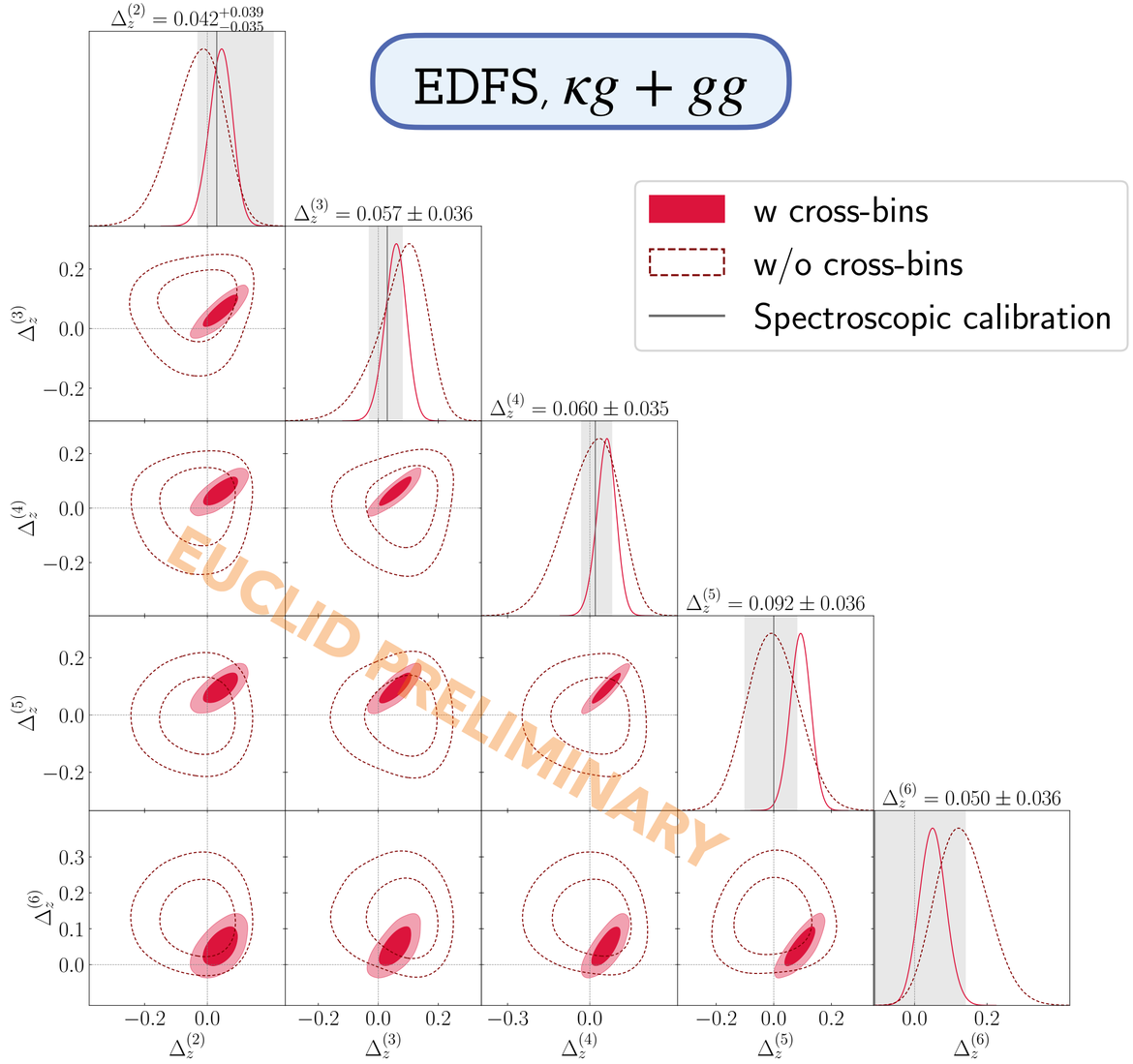
galaxy bias amplitudes

MCMC runs:

gg vs $\kappa g + gg$, each with and without g cross-bins for

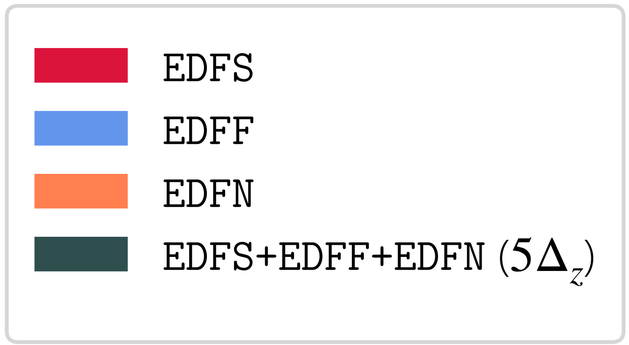
- ✓ each field separately
- ✓ joint fields, shared photo-z shifts (5 Δ_z)
- ✓ joint fields, per-field photo-z shifts (15 Δ_z)

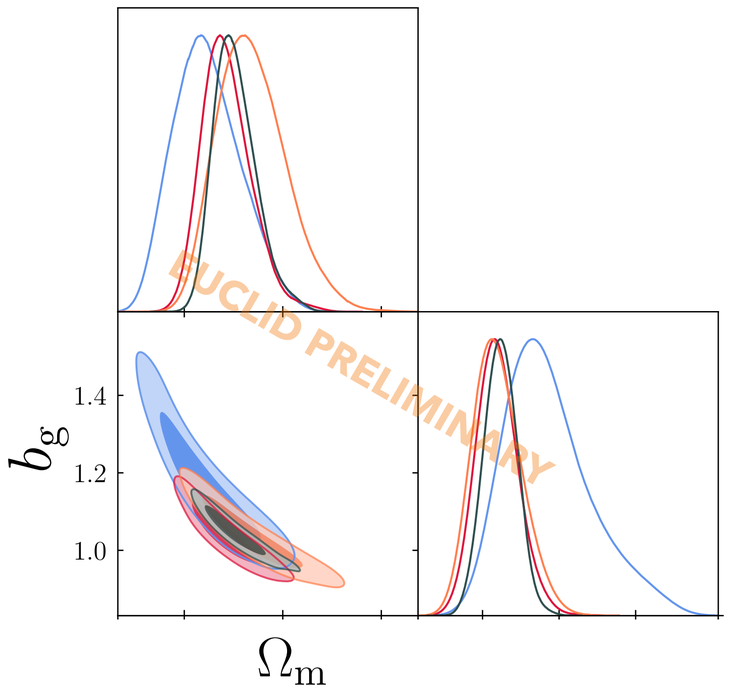
With/without cross-bins

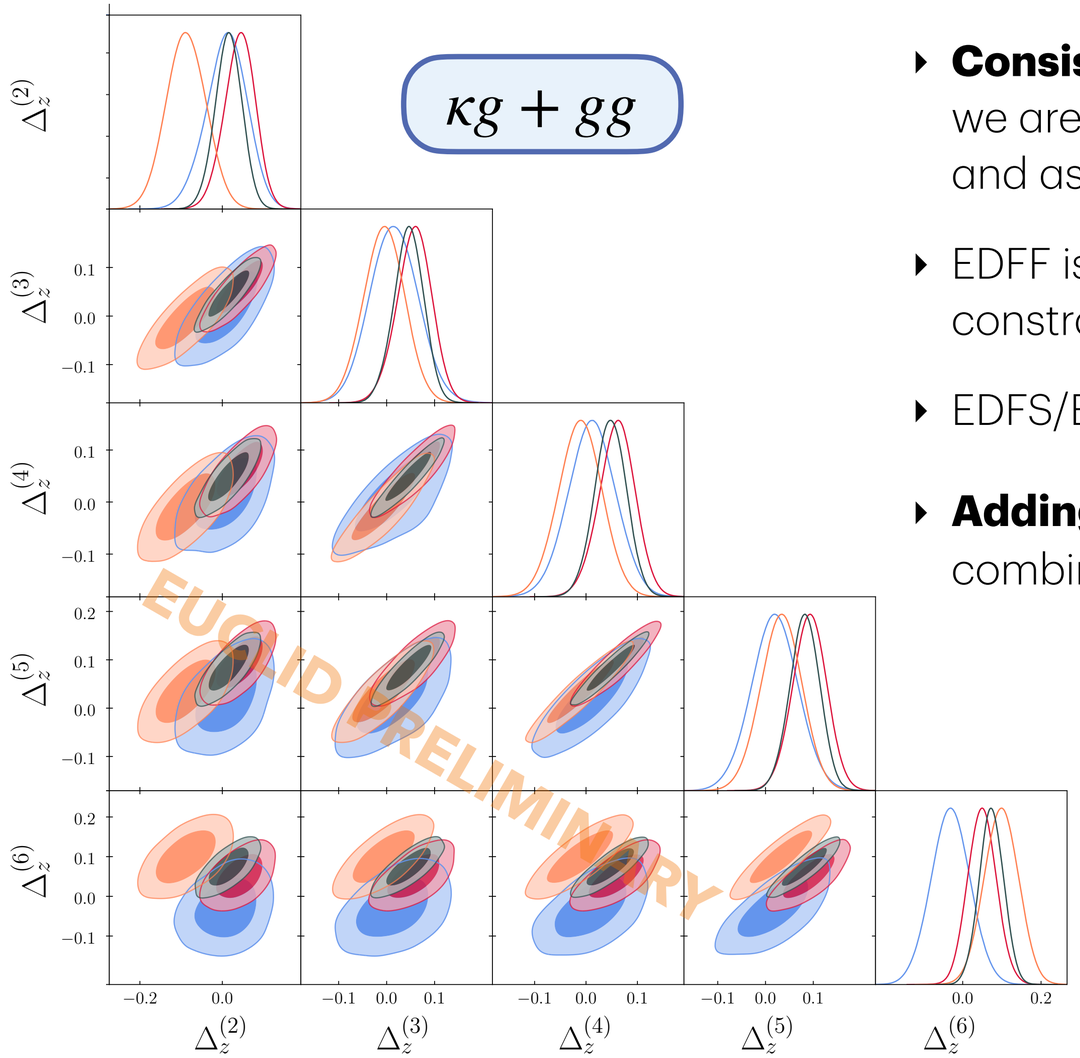


- Photo-z errors **constrained** directly **from data**
- $\sigma(\Delta_z^{(i)})$ ~2x **better than** results obtained from **spectroscopic** cross-match (Tucci+26)

Combining the 3 ED fields

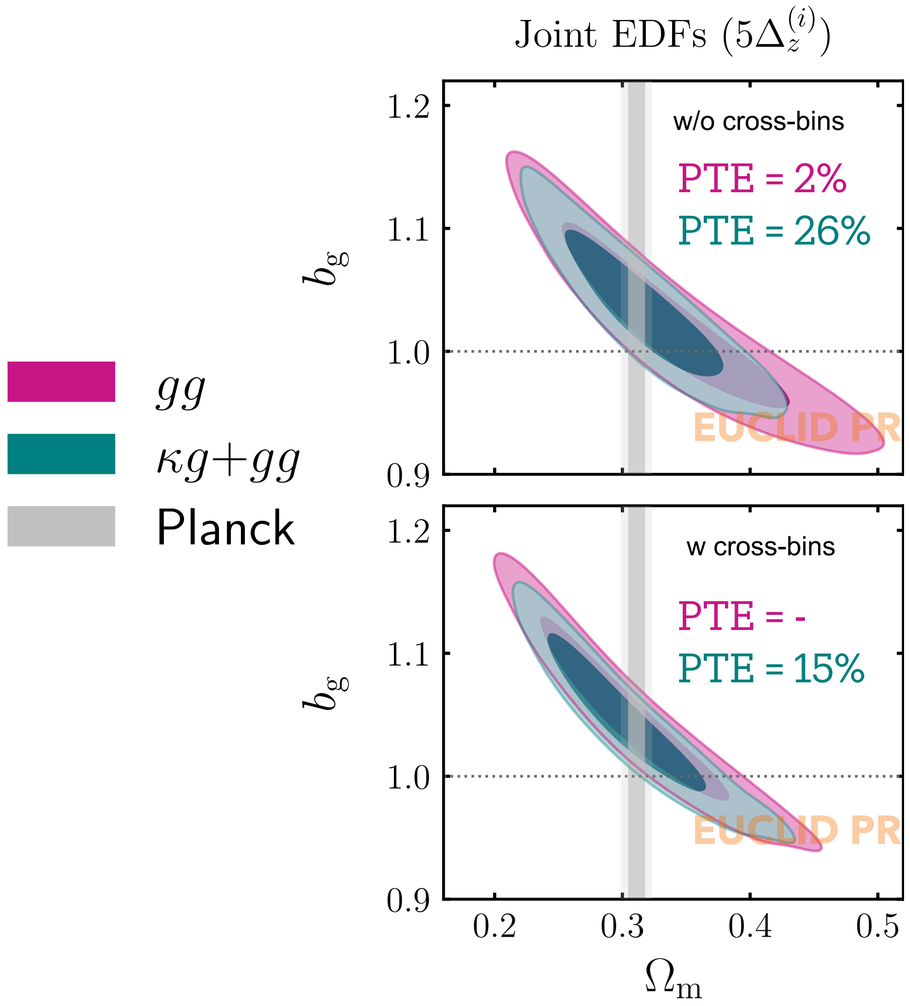






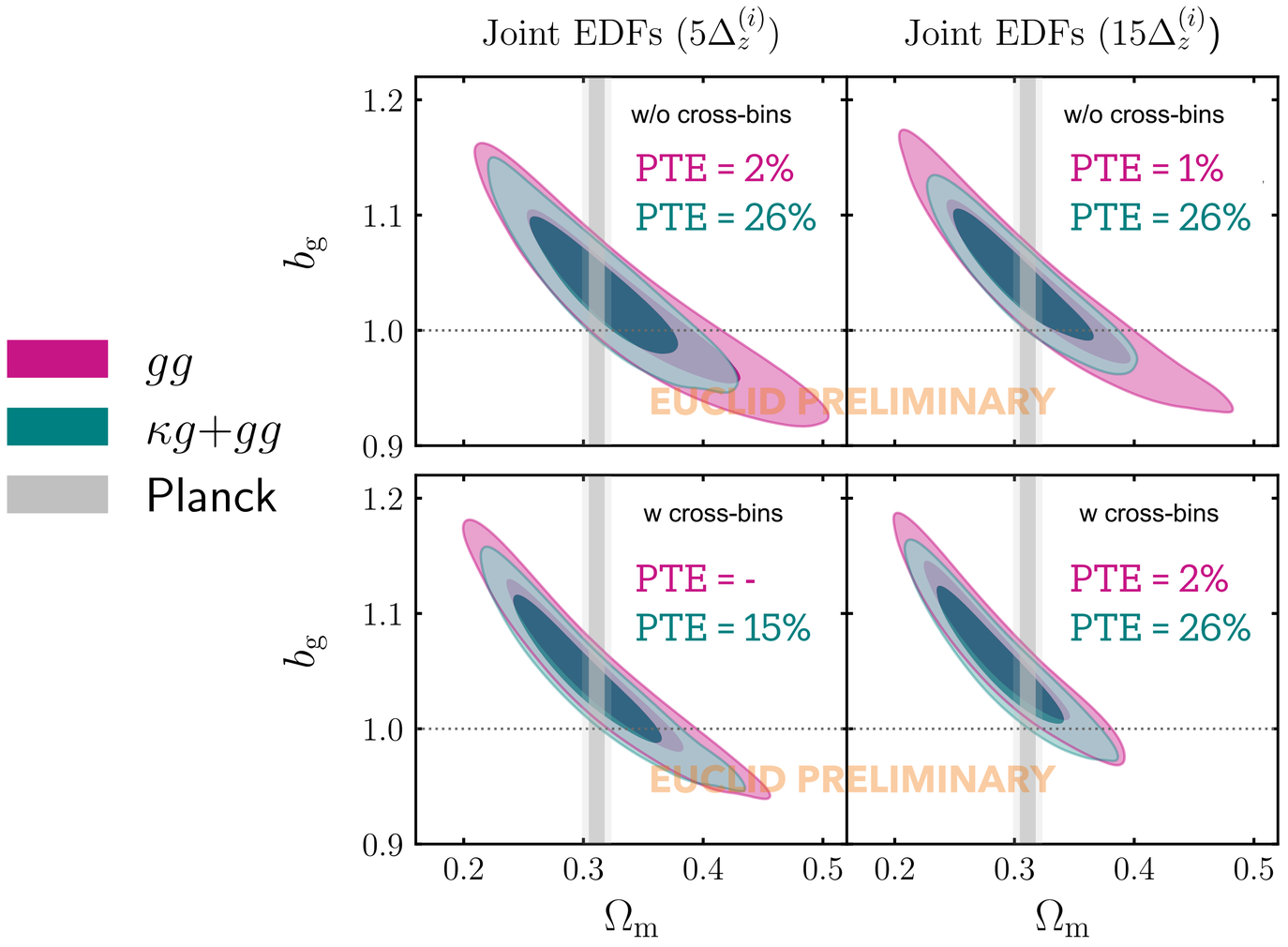
- **Consistency among the 3 fields**: we are able to model redshift errors and astrophysical nuisance coherently
- EDFF is the more problematic and less constraining
- EDFS/EDFN always slightly in tension
- **Adding κg increases the PTE** of the combined cases

The role of the κg



- $\kappa g + gg$: **equally good with or w/o cross bins**
- κg **breaks degeneracies** with galaxy bias and stabilizes photo-z modelling: **~30% improvement on cosmological parameters**

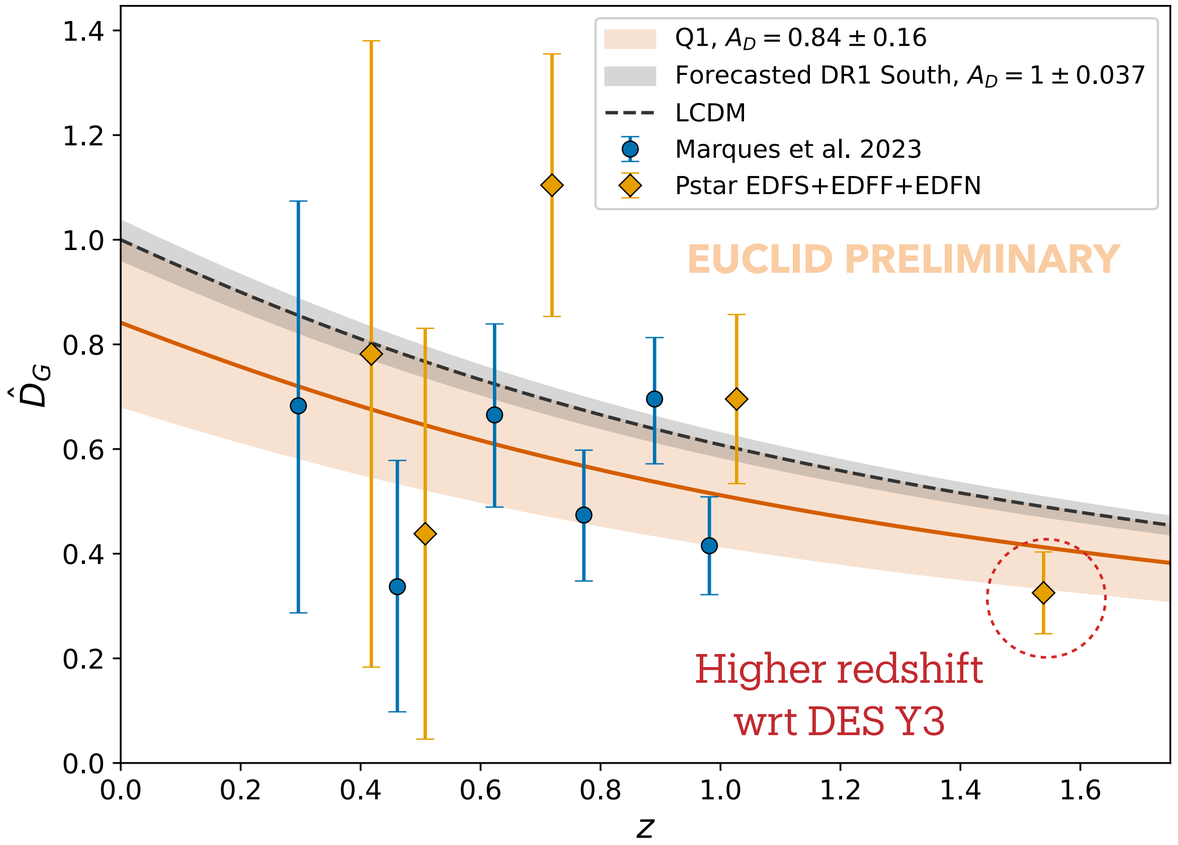
The role of the κg



- **$\kappa g + gg$: equally good with or w/o cross bins**
- **κg breaks degeneracies** with galaxy bias and stabilizes photo-z modelling: **~30% improvement on cosmological parameters**
- **15 Δ_z:** better photo-z errors handling and 15% tighter constraints

Q1 vs state of the art results (1)

Comparable to DES Y3 x ACT
with ~ x9 less sky area!



$$\hat{D}_G(z) \sim \frac{C_\ell^{\kappa g}}{\sqrt{C_\ell^{gg}}} \sim \frac{b_g D^2(z)}{\sqrt{b_g^2 D^2(z)}} = A_D D_{\rm fid}(z)$$

- **Removes naturally redshift and bias modeling uncertainties**
- Combining the 3 ED fields, we measure the amplitude of structure growth:

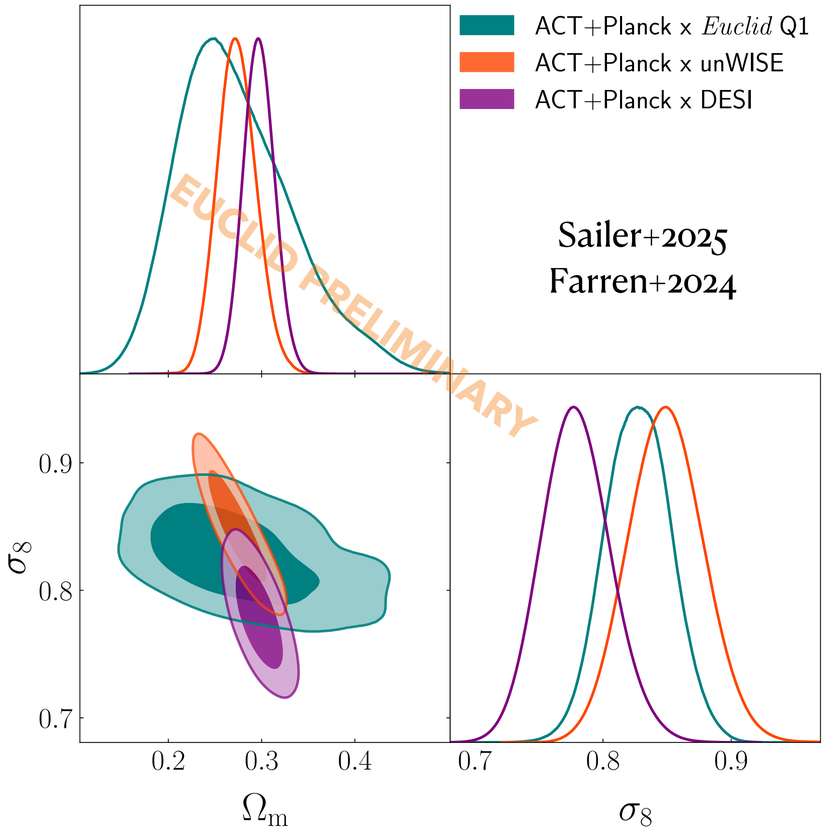
$$A_D = 0.84 \pm 0.16$$

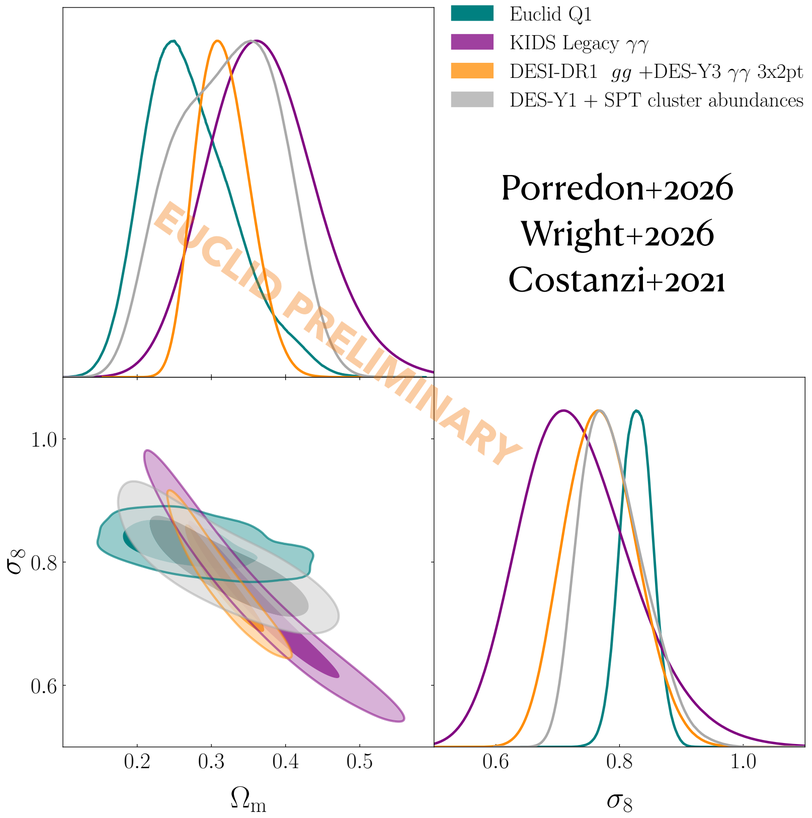
similar to the ACT x DES (Marques et al. 2023)

from 500 deg2 : $A_D = 0.87 \pm 0.14$

Q1 vs state of the art results (2)

- Adopting galaxy bias priors (conservative 3σ) from FS2 for 2x2-pt : $\sigma(\sigma_8) \sim 0.025$
- **Comparable to full unWISE/DESI x ACT+Planck** using ~10 000 deg²
- $S_8 = 0.79^{+0.07}_{-0.09}$, **comparable with current $\sigma\left(S_8\right) \sim 0.02$** accounting for sky coverage.





Conclusions

- **Euclid x CMB** will probe cosmology with unprecedented precision
- **Promising cosmology results achieved in Q1**: $\sigma(\sigma_8) = 0.025$ and $A_D = 0.84 \pm 0.16$
  - Cross-correlation almost immune to systematics and robust to photo-z errors
  - Breaking degeneracy and improve the constraining power (up to 30% on Ω_m)
- DR1-foundation in ~10 days —> **full DR1 ~June 2027**
  - With large number density and area come great responsibility!
  - We are testing a Q1-like data vector with DR1 data
    - ✓ SNR >30σ $C_\ell^{\kappa g}$ alone!
    - ✓ Minor impact of VMPZ so far
    - ✓ Ongoing tests with tomographic binning (1-10 bins)



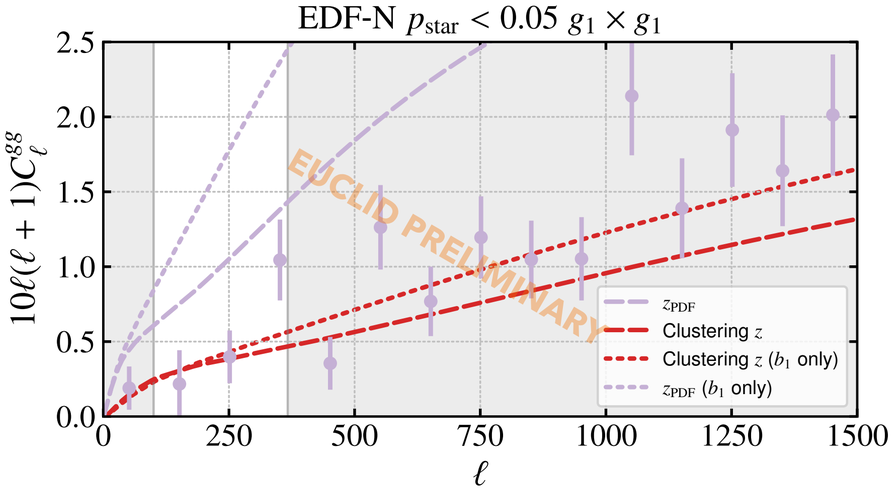
Backup slides

$n(z)$ vs spectroscopic cross-match

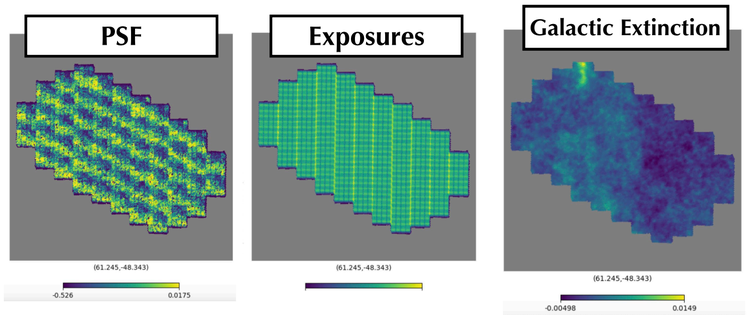
	EDF-S+EDF-F			EDF-N		
	$p_{\rm gal} > 0.90$	$p_{\rm star} < 0.05$	FS2	$p_{\rm gal} > 0.90$	$p_{\rm star} < 0.05$	FS2
$\Delta_z^{(1)}$	$0.07^{+0.44}_{-0.11}$ (0.18)	$0.07^{+0.46}_{-0.11}$ (0.21)	$0.08^{+0.36}_{-0.08}$ (0.11)	$0.06^{+0.15}_{-0.05}$ (0.07)	$0.06^{+0.08}_{-0.04}$ (0.08)	$0.08^{+0.20}_{-0.07}$ (0.09)
$\Delta_z^{(2)}$	$0.03^{+0.17}_{-0.06}$ (0.08)	$0.03^{+0.18}_{-0.06}$ (0.08)	$0.03^{+0.17}_{-0.08}$ (0.10)	$0.05^{+0.14}_{-0.05}$ (0.06)	$0.08^{+0.03}_{-0.09}$ (0.08)	$0.04^{+0.13}_{-0.08}$ (0.08)
$\Delta_z^{(3)}$	$0.03^{+0.05}_{-0.07}$ (0.05)	$0.03^{+0.05}_{-0.06}$ (0.05)	$-0.01^{+0.06}_{-0.11}$ (0.06)	$0.01^{+0.08}_{-0.07}$ (0.06)	$0.01^{+0.06}_{-0.05}$ (0.06)	$0.01^{+0.06}_{-0.08}$ (0.06)
$\Delta_z^{(4)}$	$0.02^{+0.06}_{-0.05}$ (0.05)	$0.02^{+0.06}_{-0.05}$ (0.05)	$0.01^{+0.07}_{-0.08}$ (0.06)	$0.02^{+0.07}_{-0.04}$ (0.05)	$0.03^{+0.07}_{-0.06}$ (0.05)	$0.01^{+0.07}_{-0.08}$ (0.07)
$\Delta_z^{(5)}$	$-0.01^{+0.07}_{-0.09}$ (0.08)	$0.00^{+0.08}_{-0.10}$ (0.08)	$-0.02^{+0.07}_{-0.09}$ (0.07)	$0.01^{+0.09}_{-0.08}$ (0.08)	$-0.01^{+0.10}_{-0.10}$ (0.09)	$0.01^{+0.08}_{-0.09}$ (0.07)
$\Delta_z^{(6)}$	$-0.27^{+0.22}_{-0.59}$ (0.34)	$-0.11^{+0.25}_{-0.69}$ (0.35)	$-0.04^{+0.11}_{-0.15}$ (0.11)	$-0.06^{+0.10}_{-0.28}$ (0.14)	$-0.15^{+0.19}_{-0.37}$ (0.23)	$-0.03^{+0.09}_{-0.14}$ (0.10)

In parentheses: normalised median absolute deviation

- **Priors from** comparison with FS2 and **external spectroscopic sample** used in Tucci+26
- **Bin 1** can be retrieved from clustering redshift but **discarded** in the following

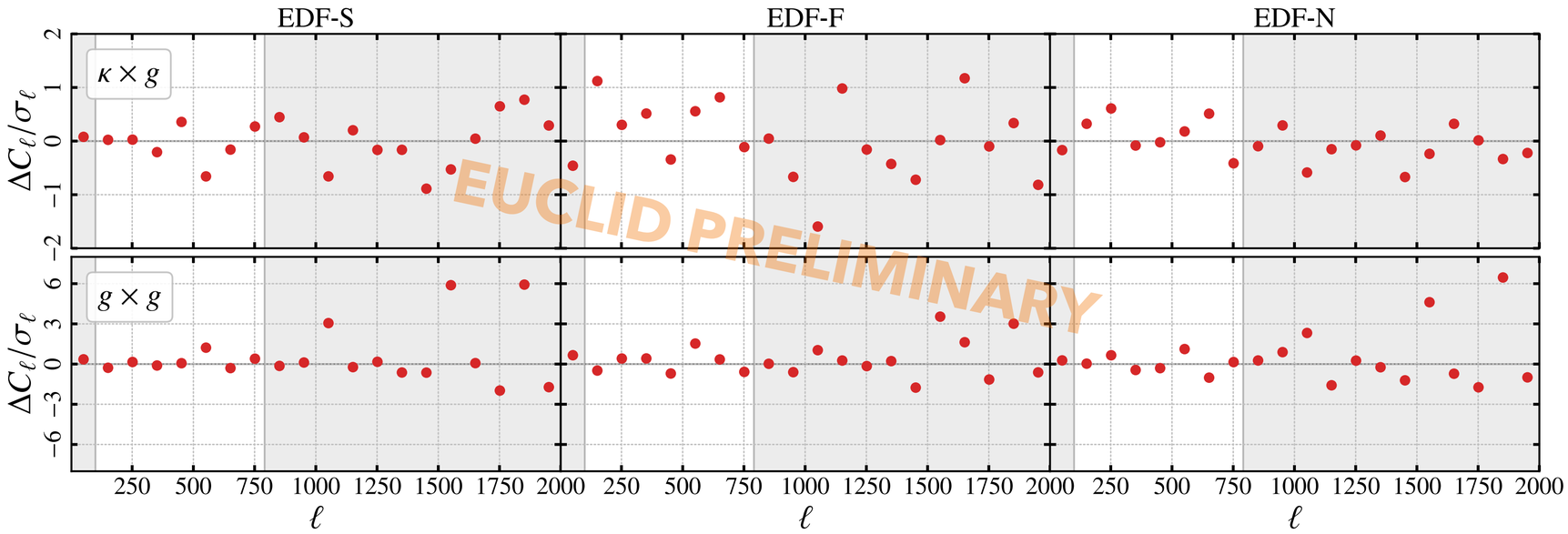


Imaging systematic treatment

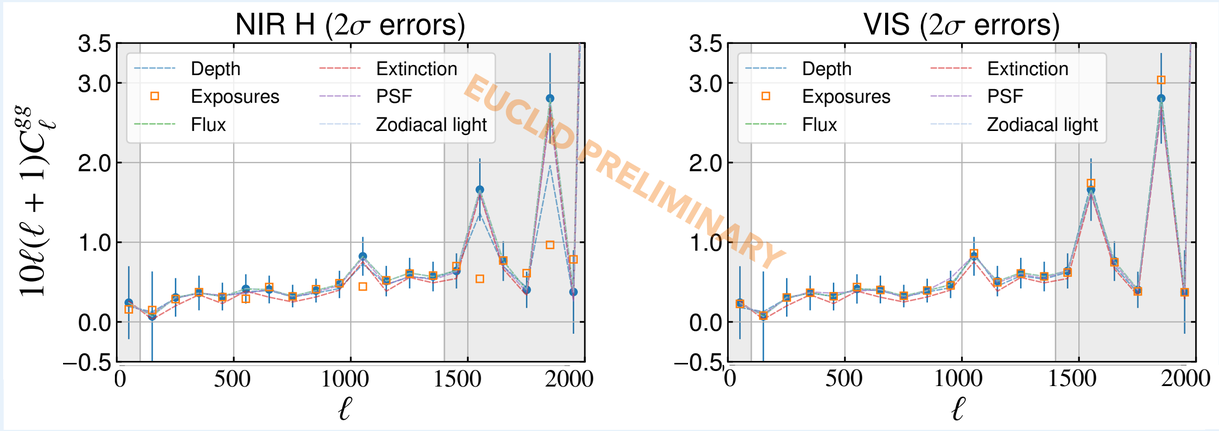


+12 others

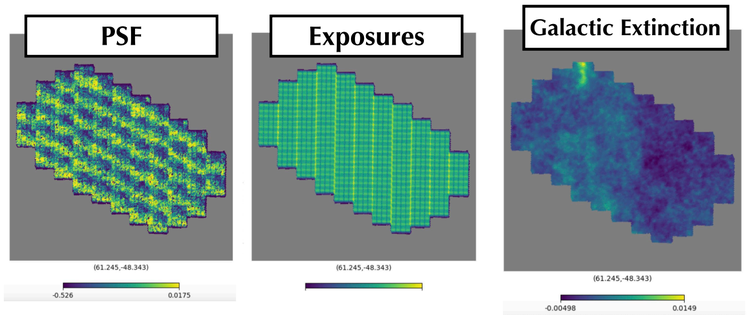
Linear deprojection



Galaxy clustering auto

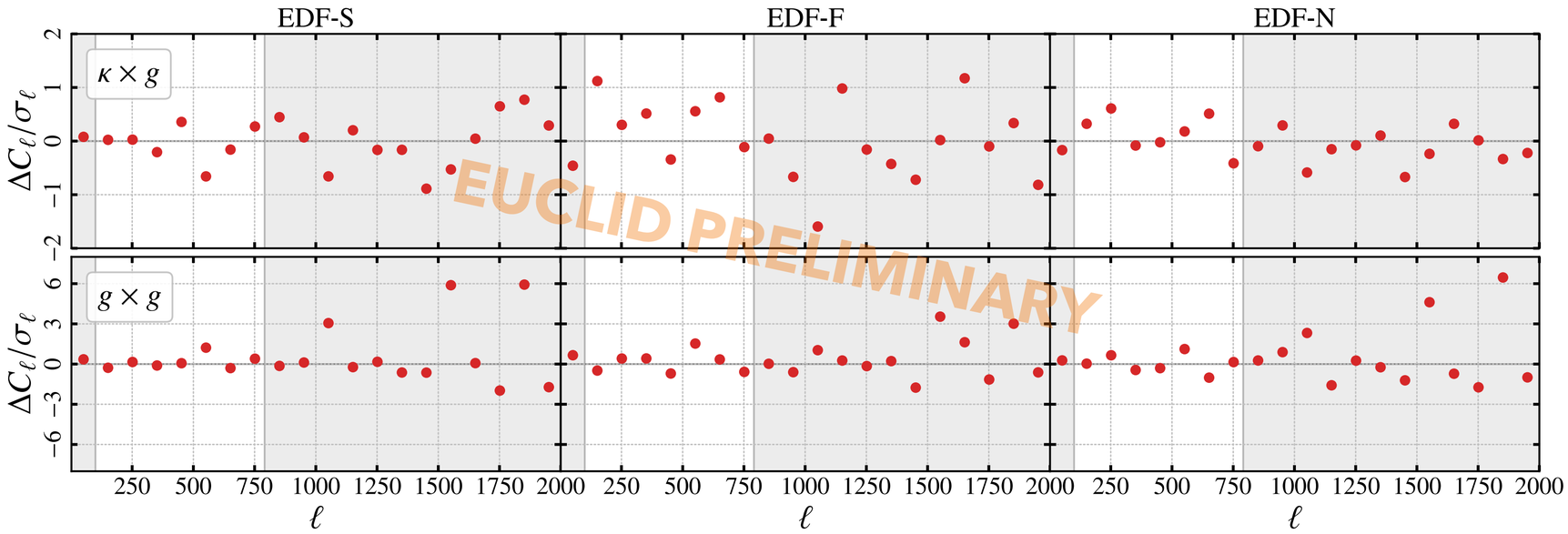


Imaging systematic treatment

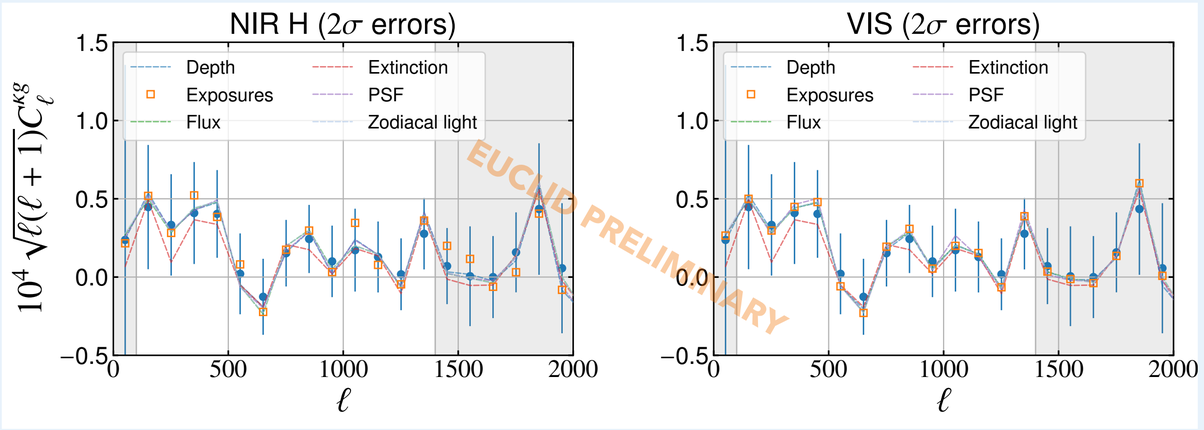


+12 others

Linear deprojection

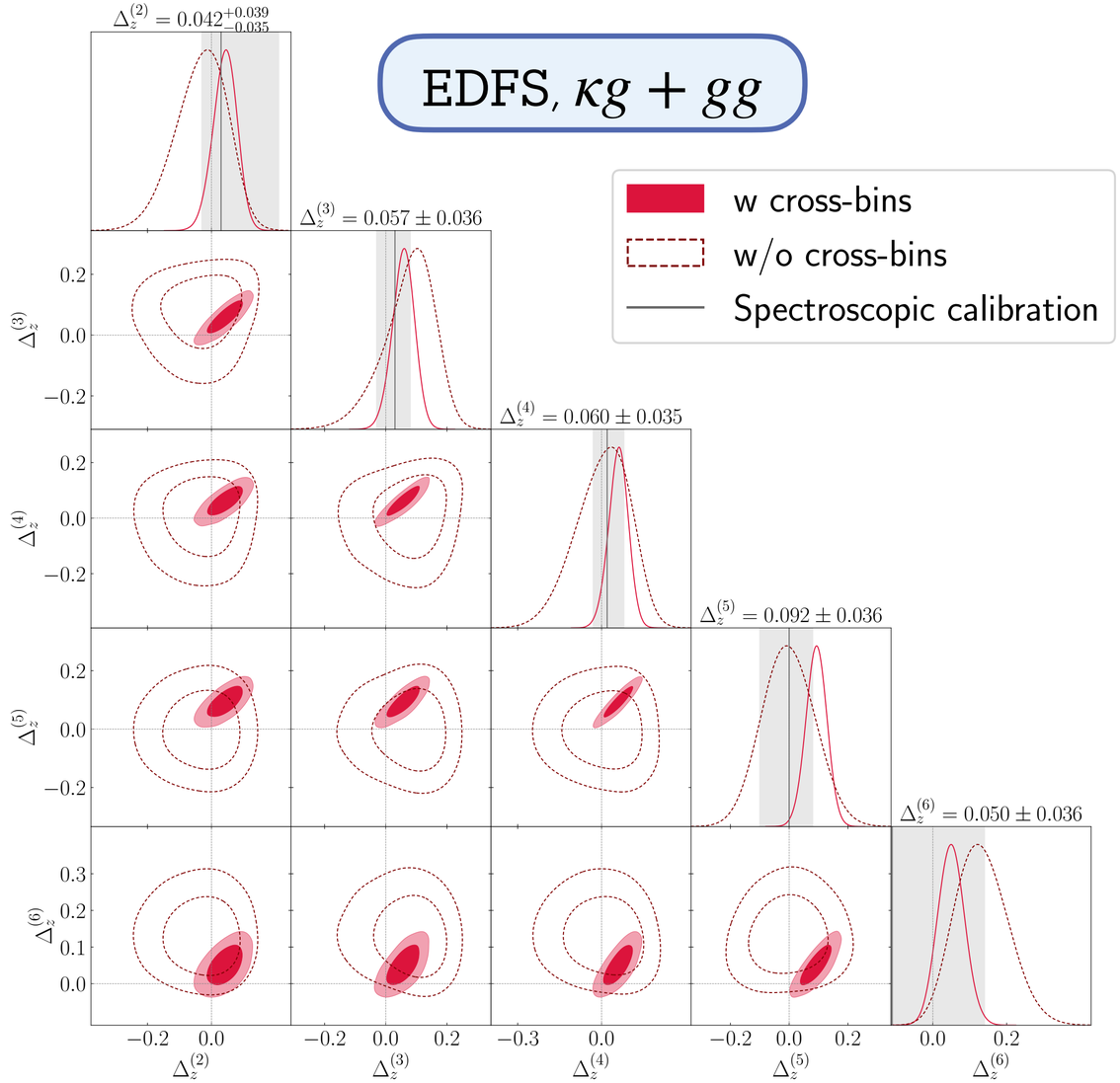


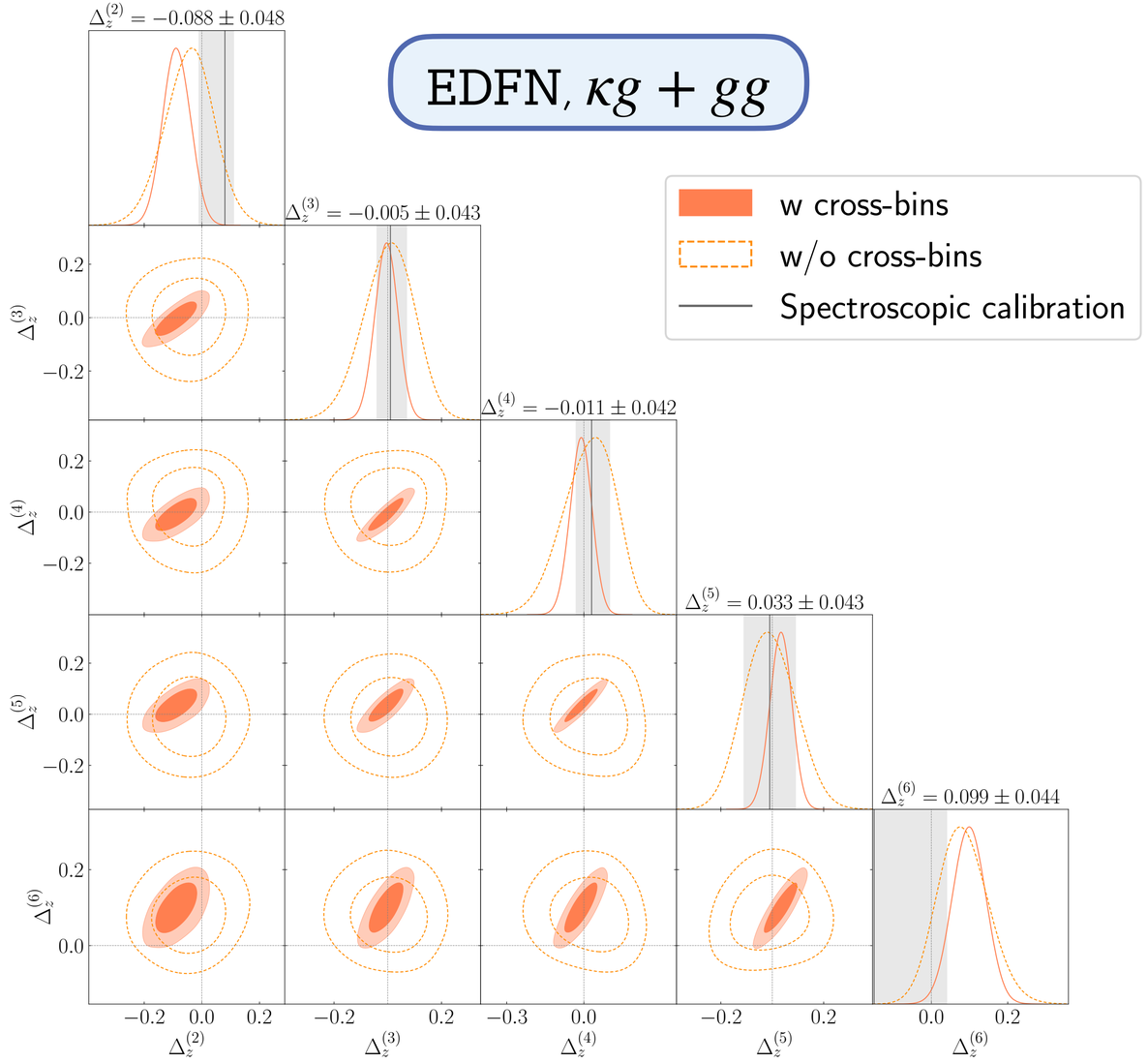
CMB lensing x galaxy clustering



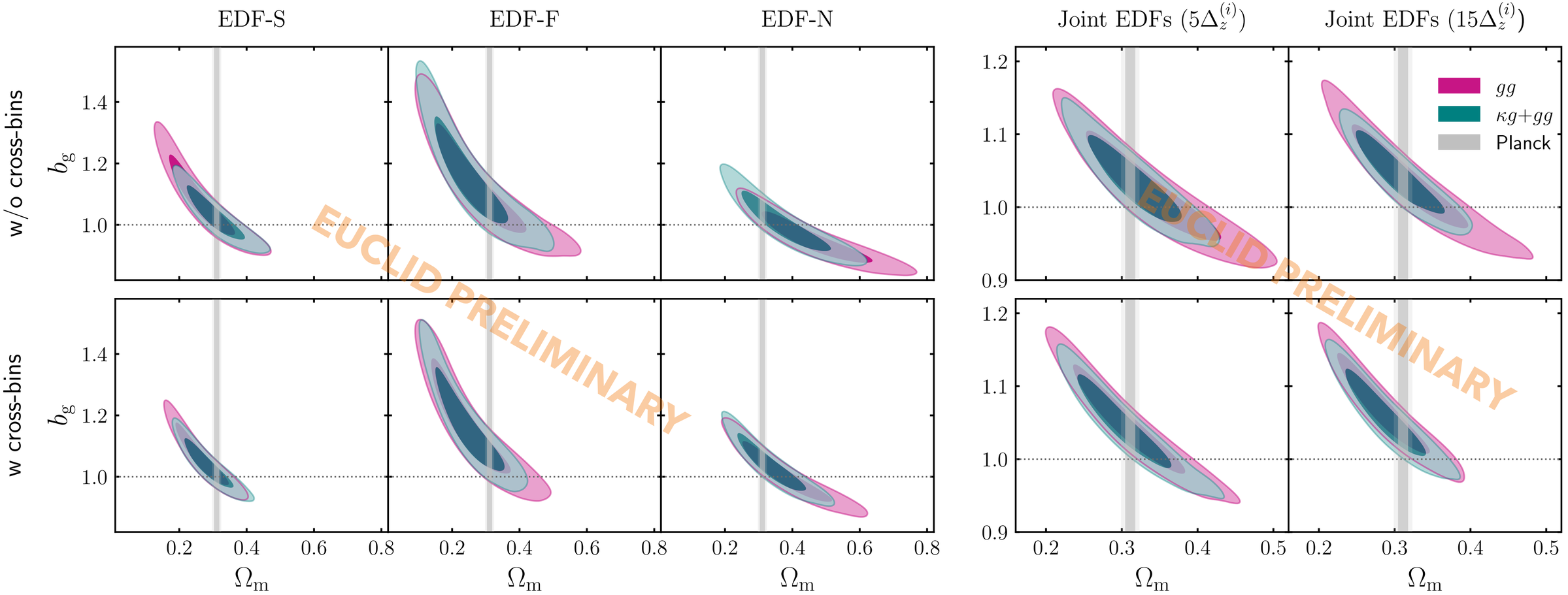
Totally immune!

With/without cross-bins





The role of the κg



Deep dive into Q1 maps

Two different sample selection based on purity of galaxy classification or star classification rejection respectively

The two cuts deliver samples with:
pgal = 11 gal/arcmin^2
pstar = 21 gal/arcmin^2

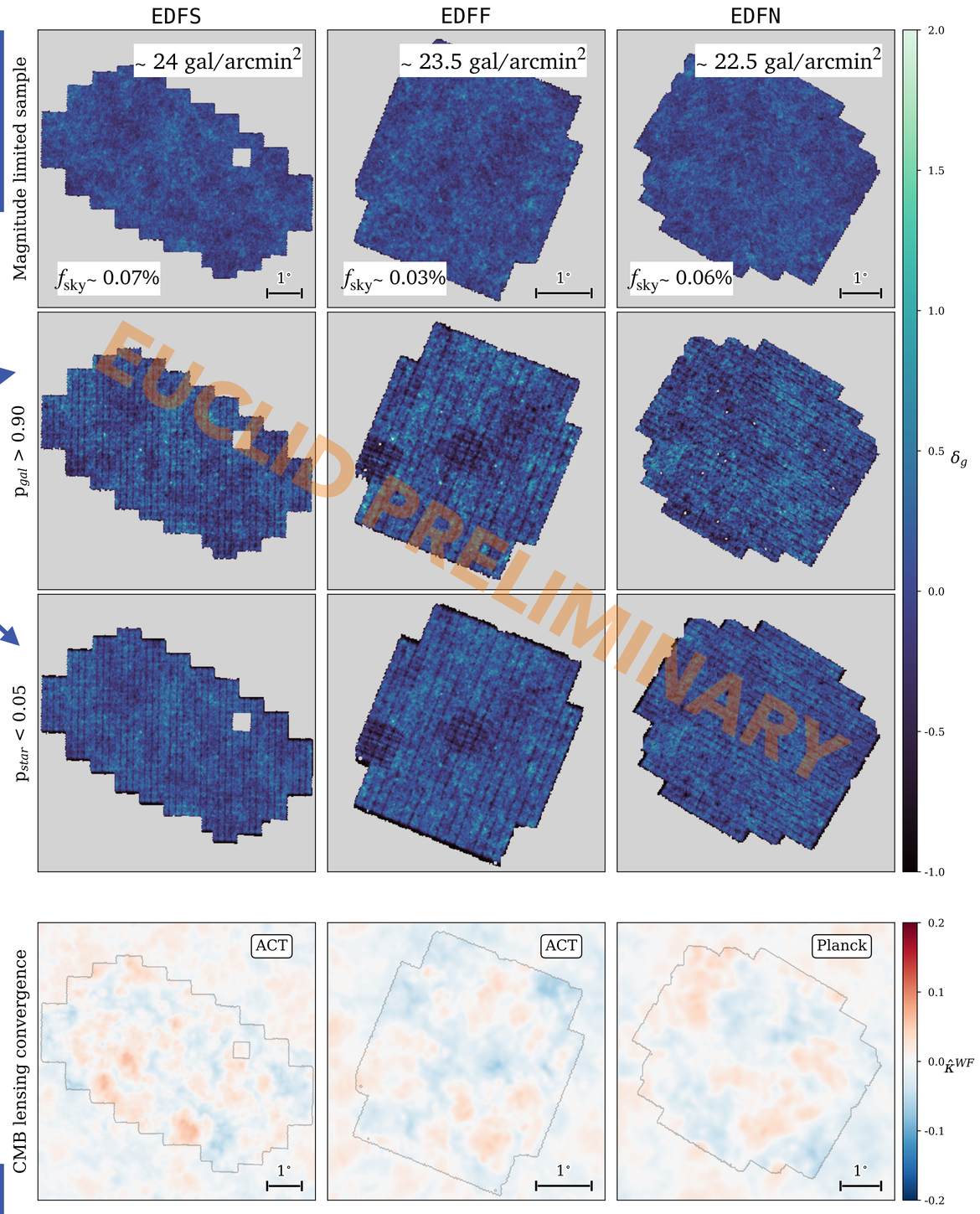
$$g \equiv \delta_g(\hat{\mathbf{n}}_p) = \frac{N(\hat{\mathbf{n}}_p)}{\bar{N} w(\hat{\mathbf{n}}_p)} - 1\,,$$

$N(\hat{\mathbf{n}}_p)$ is the number of sources in a given pixel

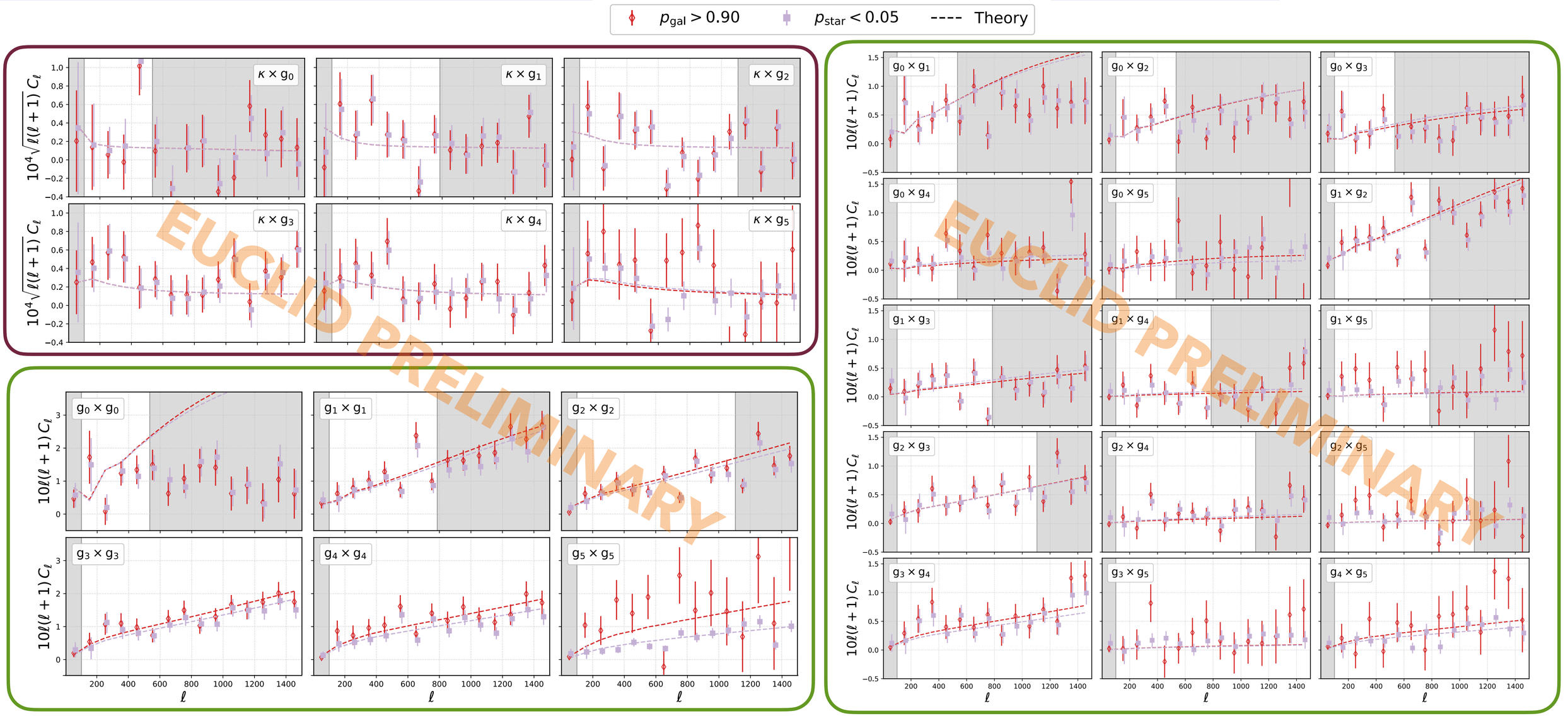
$w(\hat{\mathbf{n}}_p)$ is the value of the selection function of our galaxy sample in that same pixel

$\bar{N}$ is the mean number of galaxies per pixel, accounting for the selection function:

$$\bar{N} = \frac{\sum_p N(\hat{\mathbf{n}}_p)}{\sum_p w(\hat{\mathbf{n}}_p)}$$

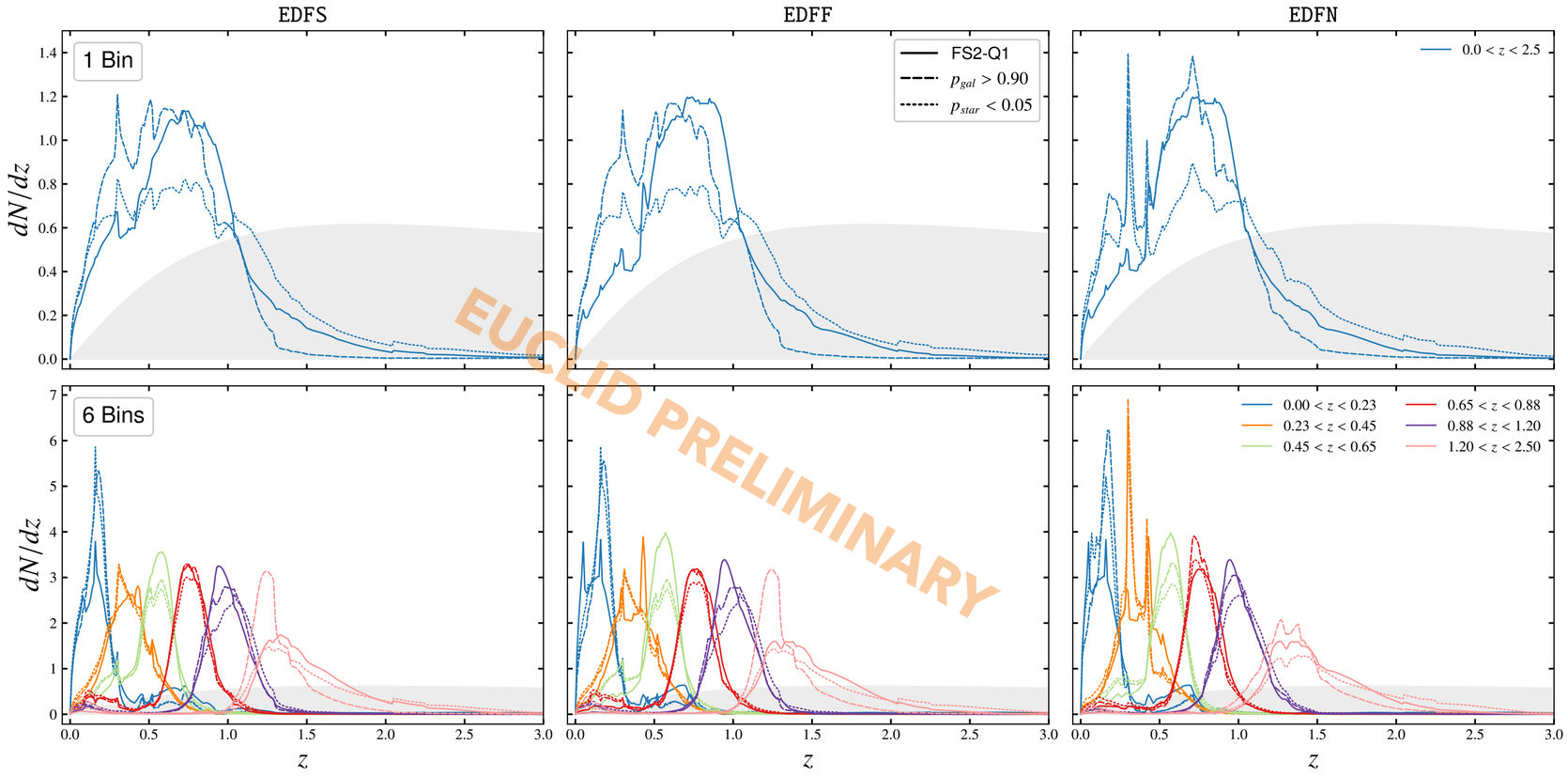


Power spectra estimation



Redshift distributions

- For each redshift bin, the $\mathrm{d}N/\mathrm{d}z$ is estimated from stacking of the galaxy's photo-z PDF
- South (EDFS) and Fornax (EDFF) are consistent, while EDFN (North) is not



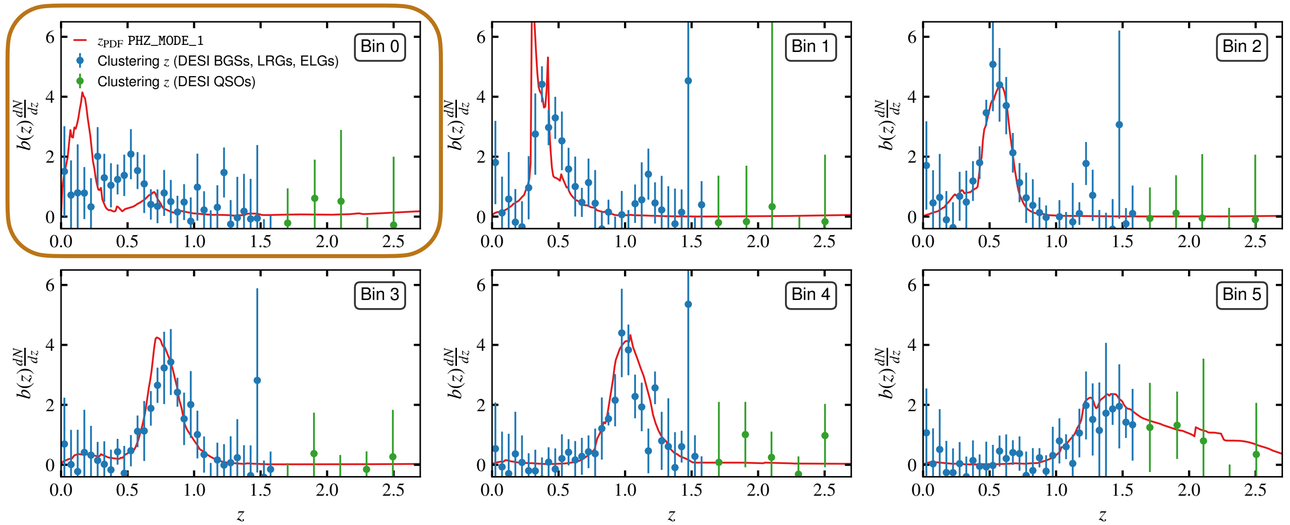
Different external photometric data:

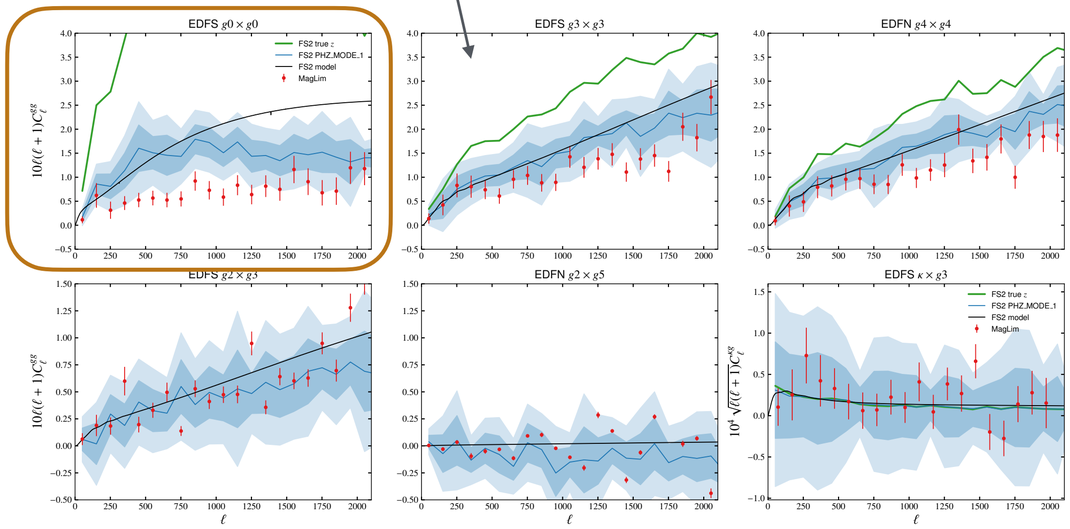
EDFN: the UNIONS survey combined with Pan-STARRS

EDFS and EDFF: DES data

Validation

- Null tests:
  - kappa x g_{null} , g_{null} x g_{null}
  - $kappa_{null}$ x g
  - x between different fields
- Consistency with clustering redshifts
- Consistency with tomographic Flagship2 simulation





Robustness tests

$$\bar{\sigma} = \frac{\mu_{\rm sub} - \mu_{\rm full}}{\sqrt{\left|\sigma^2_{\rm sub} - \sigma^2_{\rm full}\right|}}$$

Compatibility $\kappa g + gg$ vs gg

Field	Cross-bins	$\Omega_{\rm m}$	$b_{\rm g}$
EDF-S	…	−1.17	0.76
	✓	−1.10	0.71
EDF-F	…	0.51	−0.90
	✓	0.33	−0.03
EDF-N	…	1.32	−1.47
	✓	0.75	−1.44

Compatibility with vs without cross-bins

Field	Data	$\Omega_{\rm m}$	$b_{\rm g}$	$\Delta_z^{(2)}$	$\Delta_z^{(3)}$	$\Delta_z^{(4)}$	$\Delta_z^{(5)}$	$\Delta_z^{(6)}$
EDF-S	gg	0.01	0.33	−0.99	−0.03	−0.58	−1.04	0.98
	κg+gg	0.71	−0.37	−1.04	0.26	−0.62	−1.15	1.34
EDF-F	gg	0.60	−0.86	−0.96	1.17	−0.77	−0.33	1.10
	κg+gg	0.25	−0.21	−0.93	1.21	−0.80	−0.27	1.00
EDF-N	gg	1.37	−1.54	0.66	0.06	0.22	−0.57	0.10
	κg+gg	0.70	−1.89	0.64	0.10	0.35	−0.46	−0.32

Leave-one-out (LOO) compatibility

		LOO bin 2		LOO bin 3		LOO bin 4		LOO bin 5		LOO bin 6	
Field	Data	$\Omega_{\rm m}$	$b_{\rm g}$	$\Omega_{\rm m}$	$b_{\rm g}$	$\Omega_{\rm m}$	$b_{\rm g}$	$\Omega_{\rm m}$	$b_{\rm g}$	$\Omega_{\rm m}$	$b_{\rm g}$
EDF-S	gg	−0.30	…	0.39	−0.79	…	−0.95	0.40	−0.72	…	1.09
	κg+gg	…	0.41	1.03	−1.58	…	−1.15	…	…	0.02	0.49
EDF-F	gg	−0.41	…	0.87	$3.01^{\dagger}$	−0.09	1.19	0.25	−1.08	0.46	−0.04
	κg+gg	−0.55	0.71	0.92	$-3.17^{\dagger}$	−0.34	1.16	…	−1.09	−0.03	0.34
EDF-N	gg	−0.94	1.04	…	−0.29	−0.42	−0.27	0.92	−1.31	0.02	0.42
	κg+gg	−0.69	1.31	0.13	−0.44	−0.41	−0.24	0.94	−1.37	−0.35	0.58

Cosmological inference

Field	Data	Cross-bins	Ω_m	b_g	PTE
EDF-S	gg	✓	$0.26^{+0.05}_{-0.06}$	$1.07^{+0.06}_{-0.08}$	0.35
	κg+gg	✓	$0.29^{+0.04}_{-0.06}$	$1.04^{+0.05}_{-0.06}$	0.15
	gg	...	$0.27^{+0.05}_{-0.08}$	$1.08^{+0.08}_{-0.10}$	0.48
	κg+gg	...	$0.31^{+0.05}_{-0.07}$	$1.03^{+0.05}_{-0.07}$	0.08
EDF-F	gg	✓	$0.26^{+0.04}_{-0.11}$	$1.17^{+0.12}_{-0.14}$	0.31
	κg+gg	✓	$0.25^{+0.06}_{-0.08}$	$1.17^{+0.08}_{-0.13}$	0.26
	gg	...	$0.28^{+0.06}_{-0.11}$	$1.13^{+0.09}_{-0.15}$	0.05
	κg+gg	...	$0.25^{+0.06}_{-0.09}$	$1.16^{+0.09}_{-0.14}$	0.23
EDF-N	gg	✓	$0.38^{+0.08}_{-0.10}$	$1.01^{+0.06}_{-0.08}$	0.01
	κg+gg	✓	$0.34^{+0.06}_{-0.08}$	$1.04^{+0.06}_{-0.07}$	0.81
	gg	...	$0.46^{+0.09}_{-0.13}$	$0.96^{+0.05}_{-0.07}$	0.01
	κg+gg	...	$0.38^{+0.07}_{-0.11}$	$1.00^{+0.05}_{-0.08}$	0.84
Joint EDFs (5 $\Delta_z^{(i)}$)	gg	✓	$0.31^{+0.04}_{-0.06}$	$1.05^{+0.05}_{-0.06}$	<0.01
	κg+gg	✓	$0.30^{+0.04}_{-0.05}$	$1.05^{+0.04}_{-0.04}$	0.15
	gg	...	$0.34^{+0.05}_{-0.07}$	$1.02^{+0.04}_{-0.06}$	0.02
	κg+gg	...	$0.32^{+0.04}_{-0.05}$	$1.033^{+0.035}_{-0.043}$	0.26
Joint EDFs (15 $\Delta_z^{(i)}$)	gg	✓	$0.29^{+0.04}_{-0.05}$	$1.07^{+0.04}_{-0.05}$	0.02
	κg+gg	✓	$0.29^{+0.03}_{-0.04}$	$1.06^{+0.04}_{-0.04}$	0.26
	gg	...	$0.32^{+0.04}_{-0.06}$	$1.04^{+0.05}_{-0.05}$	0.01
	κg+gg	...	$0.31^{+0.03}_{-0.05}$	$1.04^{+0.04}_{-0.04}$	0.26

Marginalised cosmological parameters obtained using different data set combinations of Euclid Q1 $p_{\rm star}$ galaxy sample and CMB lensing from ACT and Planck.

The corresponding *p*-value of the best fit is in the last column

Comparison with Planck cosmology

Field	Data	z bins	Cross-bins	$p_{gal} > 0.90$		$p_{star} < 0.05$	
				PTE	S/N	PTE	S/N
EDF-S	gg	6	✓	0.44	26	0.00	32
	κg+gg		✓	0.13	27	0.00	32
	gg	6	...	0.09	24	0.01	27
	κg+gg		...	0.25	25	0.00	30
	gg	3	✓	0.76	22	0.12	22
	κg+gg		✓	0.44	22	0.03	23
EDF-F	gg	6	✓	0.01	16	0.71	20
	κg+gg		✓	0.99	17	0.94	20
	gg	6	...	0.17	16	0.27	19
	κg+gg		...	0.29	16	0.48	19
	gg	3	✓	0.62	14	0.57	14
	κg+gg		✓	0.51	14	0.78	14
EDF-N	gg	6	✓	0.00	23	0.00	29
	κg+gg		✓	0.00	23	0.00	29
	gg	6	...	0.11	21	0.29	26
	κg+gg		...	0.19	21	0.20	26
	gg	3	✓	0.02	19	0.02	20
	κg+gg		✓	0.01	19	0.00	20

Summary of PTE between our fiducial theoretical predictions and measurements obtained for all the Euclid Q1 fields and galaxy samples considered in this work